
Engineered nanomaterial interactions with bilayer lipid membranes: screening platforms to assess nanoparticle toxicity

Alexander Negoda and Ying Liu

Department of Chemical Engineering and Material Science,
Michigan State University,
2527 Engineering Building,
East Lansing, MI 48824-1226, USA
Fax: 517-432-1105
E-mail: negoda@msu.edu
E-mail: liuying7@egr.msu.edu

Wen-Che Hou

School of Sustainable Engineering and the Built Environment,
Arizona State University,
Tempe, AZ 85287, USA
E-mail: hou.wen-che@epamail.epa.gov

**Charlie Corredor and
Babak Yaghoubi Moghadam**

Chemical Engineering and Materials Science Department,
University of Washington,
Seattle, WA 98195, USA
E-mail: corredor@uw.edu
E-mail: babakym@uw.edu

Corey Musolff

Department of Physics and Astronomy,
Michigan State University,
East Lansing, MI, 48824, USA
E-mail: musolffc@msu.edu

Lin Li

Department of Electrical and Computer Engineering,
Michigan State University,
East Lansing, MI, 48824, USA
E-mail: lili1@msu.edu

William Walker

Chemical Engineering and Materials Science Department,
University of Washington,
Seattle, WA 98195, USA
E-mail: walkew@uw.edu

Paul Westerhoff

School of Sustainable Engineering and the Built Environment,
Arizona State University,
Tempe, AZ 85287, USA
E-mail: p.westerhoff@asu.edu

Andrew J. Mason

Department of Electrical and Computer Engineering,
Michigan State University,
East Lansing, MI, 48824, USA
E-mail: mason@egr.msu.edu

Phillip Duxbury

Department of Physics and Astronomy,
Michigan State University,
East Lansing, MI, 48824, USA
E-mail: duxbury@pa.msu.edu

Jonathan D. Posner

Chemical Engineering and Materials Science Department,
University of Washington,
Seattle, WA 98195, USA
E-mail: jposner@uw.edu

R. Mark Worden*

Department of Chemical Engineering and Material Science,
Michigan State University,
2527 Engineering Building,
East Lansing, MI 48824-1226, USA
Fax: 517-432-1105
E-mail: worden@egr.msu.edu
*Corresponding author

Abstract: Engineered nanomaterials (ENMs) have attractive functional properties and are increasingly being used in commercial products. However, ENMs present health risks that are poorly understood and difficult to assess. Because ENMs must interface with cell membranes to cause biological effects, improved methods are needed to measure ENM-biomembrane interactions. The goals of this paper are to review the current status of methods to characterise interactions between ENMs and bilayer lipid membranes that mimic cell membranes, and to present example applications of the methods relevant to nanotoxicology. Four approaches are discussed: electrochemical methods that measure ENM-induced ion leakage through lipid bilayers, optical methods that measure dye leakage from liposomes, partitioning methods that measure ENM distribution coefficients between aqueous solution and immobilised lipid bilayers, and theoretical models capable of predicting fundamental molecular interactions between ENMs and biomembranes. For each approach, current literature is summarised, recent results are given, and future prospects are analysed, including the potential to be used in a high-throughput mode. The relative advantages of the various approaches are discussed, along with their synergistic potential to provide multi-dimensional characterisation of ENM-biomembrane interactions for robust health risk assessment algorithms.

Keywords: nanoparticle toxicity; nanotechnology; bilayer lipid membrane; particle physiology; impedance spectroscopy; pore; fluorescence; nanoparticle partitioning; model; high-throughput.

Reference to this paper should be made as follows: Negoda, A., Liu, Y., Hou, W-C., Corredor, C., Moghadam, B.Y., Musolff, C., Li, L., Walker, W., Westerhoff, P., Mason, A.J., Duxbury, P., Posner, J.D. and Worden, R.M. (2013) 'Engineered nanomaterial interactions with bilayer lipid membranes: screening platforms to assess nanoparticle toxicity', *Int. J. Biomedical Nanoscience and Nanotechnology*, Vol. 3, Nos. 1/2, pp.52–83.

Biographical notes: Alexander Negoda holds a PhD in Biophysics and is a Research Associate at the Department of Chemical Engineering and Materials Science, Michigan State University. Recently, his research interest is focused on the interactions of nanoparticles and biological membranes.

Ying Liu is PhD candidate and Research Assistant in the Department of Chemical Engineering and Materials Science, Michigan State University. Her research interests are focused on bio-nanotechnology and on studying of nanoparticles activity against biomimetic membranes.

Wen-Che Hou is an Assistant Research Scientist in the School of Sustainable Engineering and the Built Environment at the Arizona State University. His research interests are in the fields of implications and applications of sustainable nanotechnology as well as aquatic chemistry.

Charlie Corredor is a chemical engineering PhD candidate and Research Assistant at the University of Washington. In 2010, he was awarded with the National Academies Ford predoctoral graduate research fellowship. His current research interest is focused on nanotoxicology of engineered nanomaterials.

Babak Yaghoubi Moghadam is mechanical engineering PhD candidate and Research Assistant at the University of Washington. His research interests are focused on the development of in vitro nanotoxicology assays.

Corey Musolff is a PhD student in the Michigan State University Physics and Astronomy Department. His research interests include multi-scale modelling of molecular interactions between nanoparticles and lipid bilayers.

Lin Li is a PhD candidate in Electrical Engineering at Michigan State University (MSU), East Lansing, Michigan, USA. In 2008, he joined the Advanced Microsystems and Circuits Laboratory at MSU as a Research Assistant. His PhD research includes CMOS on-chip electrochemical biosensor arrays, CMOS packaging, and microfluidics.

William Walker is a bioengineering undergraduate Research Assistant at the University of Washington. His research interests include applications of nanotechnology in medicine.

Paul Westerhoff is a Professor in the School of Sustainable Engineering and The Built Environment at Arizona State University. His research interests are in the field of emerging pollutants in aquatic systems.

Andrew J. Mason is an Associate Professor in the Department of Electrical and Computer Engineering at Michigan State University, East Lansing, Michigan. His research spans mixed-signal circuit design and microfabrication for integrated microsystems, including low-power bioelectrochemical interrogation circuits, adaptive chemical sensor interface circuits, post-CMOS fabrication of electrochemical sensor arrays, and signal processing circuits for implantable devices.

Phillip Duxbury is a Professor of Condensed Matter Theory at Michigan State University. His research interests include theoretical modelling of nanoscale phenomena, such as interaction of nanoparticles with lipid bilayers.

Jonathan D. Posner is an Associate Professor of Mechanical Engineering at University of Washington with courtesy appointments in Chemical Engineering at UW and the Consortium for Science Policy and Outcomes at Arizona State University. His research area is micro and nanoscale transport phenomena at the intersection of chemistry, biology, and medicine.

R. Mark Worden is a Professor in the Chemical Engineering and Materials Science Department at Michigan State University. His research interests lie at the intersection of biotechnology and nanotechnology and include biocatalysis, interactions of nanomaterials with living systems, and biomimetic interfaces that express biological activity.

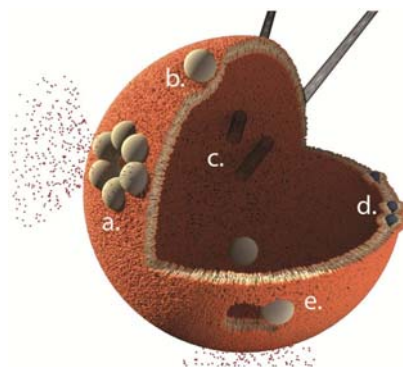
1 Introduction and scope

Engineered nanomaterials (ENMs) have unique and desirable functional properties due to their extremely small size (between 1 and 100 nm). As a result, ENMs have enormous economic potential and are reported in over 1,300 commercial products. However, recent reviews have summarised compelling evidence that ENMs can induce health risks (Nel et al., 2006; Buzea et al., 2007). ENMs can travel throughout the body, triggering health problems through a number of mechanisms, including denaturing proteins, compromising membranes, damaging DNA, inducing granuloma formation, increasing oxidative stress, and triggering immune responses. The difficulty in assessing the variety of potential toxic

effects induced by ENMs is compounded by the large number of ENM variations, including size, shape, composition, charge, surface functionality, etc. Consequently, it is crucial to develop high-throughput methods that can be used to predict health risks of ENMs to achieve the goal of responsible, nanoenabled technologies.

Toxicity of ENMs is commonly investigated using animal (*in-vivo*) (Li et al., 2010) and/or cell-culture (*in-vitro*) (Hsiao and Huang, 2011; Klaassen, 2007) approaches. Common toxicity endpoints in animal studies include mortality, changes in body weight, histopathology of tissue samples, inflammation markers (e.g., cytokines), and immune-cell composition in bronchoalveolar lavage fluid. Common toxicity endpoints in cell studies include cell viability (e.g., by MTS assay), cell proliferation, lactate dehydrogenase activity, histological analysis of cytokines and other markers of immune response, DNA mutation frequency, expression of genes in toxicity-associated pathways, and reactive oxygen species (ROS) levels. The molecular chain of events leading to these toxicity endpoints typically involves interactions between the ENMs and cell membranes. Lipid bilayers surround most living cells and organelles, incorporate a variety of functional membrane proteins, and constitute a continuous barrier to the transport of ions and other molecules (Alberts, 2002). Because molecules or nanoparticles must first interface with lipid bilayers to cause biological effects (Nel et al., 2009), understanding how ENMs interact with this barrier is critical to understanding cellular damage mechanisms.

Figure 1 Schematic showing diverse ENM interactions with a BLM (in form of a liposome), including (a) aggregation in the bilayer forming a disruptive nanopore, (b) adsorption to and potential deformation and modification of phase behaviour of bilayer, (c) penetration and disruption of bilayer by high aspect ratio ENMs (i.e., carbon nanotubes), (d) partitioning of ENMs into the hydrophobic core of the bilayer, and (e) disruption of bilayer and formation of nanopore, potentially leading to increased permeability to molecules and ENMs (see online version for colours)



Note: The small red dots emanating from the pores depict the leakage of molecules from the liposome.

Source: Adapted with permission from Moghadam et al. (2012)

When a nanoparticle approaches a cell membrane, several interactions are possible, as illustrated in Figure 1. The nanoparticle could be repelled by the membrane, adsorb onto the membrane, extract lipids from the membrane, become stably embedded within the membrane, pass through the membrane, induce pore formation in the membrane, rupture the membrane, activate a membrane-bound receptor protein, be endocytosed by the

membrane, or facilitate other forms of cellular damage (Rejman et al., 2004). Each of these interactions could lead to a different toxicological outcome. Once inside the cell, an ENM's ability to escape from membrane-enclosed endosomes or penetrate organelle membranes can lead to intracellular damage via mechanisms including DNA cleavage and disruption of mitochondrial architecture (Buzea et al., 2007).

Despite the central role of nanoparticle-biomembrane interactions in determining toxicological outcomes, this topic is poorly understood, and improved research tools capable of measuring, understanding, and predicting these interactions are needed to manage human and ecological risks from ENM. The properties of both the nanoparticle and biomembrane strongly influence their interactions. Research to elucidate the effect of an ENM's properties on its interactions with cells has recently been reviewed, with emphasis on mechanisms of ENM uptake and ultimate intracellular localisation (Verma and Stellacci, 2010).

However, the influence of biomembrane properties is difficult to study, for two reasons. First, the inherent complexity of cell membranes makes it difficult to isolate and characterise the effects of specific membrane components. Second, it is difficult to modify the composition of native biomembranes to test hypotheses about how composition influences membrane properties. These challenges can be addressed using a biomimetic approach in which a synthetic bilayer lipid membrane (BLM) having a known phospholipid composition is used to mimic a cell membrane. Model BLM have previously been shown to exhibit mechanical and electrical properties similar to those of cell membranes (Ti Tien and Ottova-Leitmannova, 2000; Mueller et al., 1962) and thus offer outstanding potential for systematically probing the role of specific membrane properties (lipid composition, charge, fluidity, etc.) on cell membrane interactions with ENM.

The goals of this paper are to describe the current status of four *ex-vivo* assay platforms that characterise interactions between ENMs and model BLM in the context of nanotoxicity, and to present example applications of the methods that illustrate their utility. Electrochemical methods that measure ENM-induced ion leakage through lipid bilayers are reviewed first, with an emphasis on two platforms: the planar BLM method, in which an unsupported BLM is formed across an orifice; and the tethered BLM, in which a BLM is supported and tethered to an electrode surface. Next, an optical method is discussed that measures leakage from artificial lipid vesicles using fluorescence spectroscopy. Then, an approach that measures ENMs binding to, or partitioning within, bilayers is described. The potential to use these four *ex-vivo* experimental platforms for high throughput screening is discussed. Finally, theoretical modelling approaches suitable to help interpret experimental results and elucidate fundamental molecular interactions between ENMs and biomembranes are described.

2 Electrochemical methods

2.1 Planar bilayer lipid membrane

The cell membrane provides an electrically insulating barrier that is impermeable to ions, enabling cells to maintain transmembrane ion gradients that are vital for survival and often used for intercellular signalling. Consequently, particles or molecules that affect ion transport across membranes may be detrimental to proper cell function. For example,

ENM-induced pore formation in leukocytes could alter intracellular ion concentrations, thus leading to altered immune cell activation, proliferation, differentiation, and effector function (Oh-Hora and Rao, 2008).

The field of electrophysiology has developed powerful research tools to characterise ion passage across BLM mediated by ion channels (Hille, 1992), lipid pores (Antonov et al., 2005), and toxins (Schonherr et al., 1994; Matile et al., 1996; Baldwin et al., 1995). The technique involves forming an unsupported, planar bilayer lipid membrane (pBLM) across a small orifice and then measuring the ionic conductance across the pBLM using electronics having a sensitivity on the order of 10 pS (Mironova et al., 1999). Planar-BLM research has elucidated a wide range of molecular phenomena that influence membrane permeability, including selectivity of the channels (Pavlov et al., 2005; Negoda et al., 2007), channel gating (Ruta et al., 2003) and other properties of channel functioning and regulation.

The high temporal resolution and sensitivity offered by the BLM method allow ENM-BLM interactions to be characterised by analysing patterns in the electrical signatures following ENM exposure. While this research approach is in its early stages of development, recent results have demonstrated its potential to characterise BLM perturbation by ENM. Inorganic semiconductor nanocrystals, quantum dots (QDs) were shown to induce ion currents through synthetic BLM (Ramachandran et al., 2005). Electric current was observed when a BLM was exposed to QDs having diameters of 2.2 to 15 nm at a nanomolar concentration. Klein et al. conducted similar experiments while imaging the bilayer using epi-fluorescence microscopy and directly observed QD aggregation on the surface of the bilayer, which remained fluid. They showed that a neutrally charged dye could pass across the bilayer only in the presence of the pore forming QDs (Klein et al., 2008). de Planque et al. (2011), using a modified pBLM technique, recently demonstrated that silica nanospheres (aminated and unfunctionalised) 50 nm to 500 nm in diameter disrupted biomembranes.

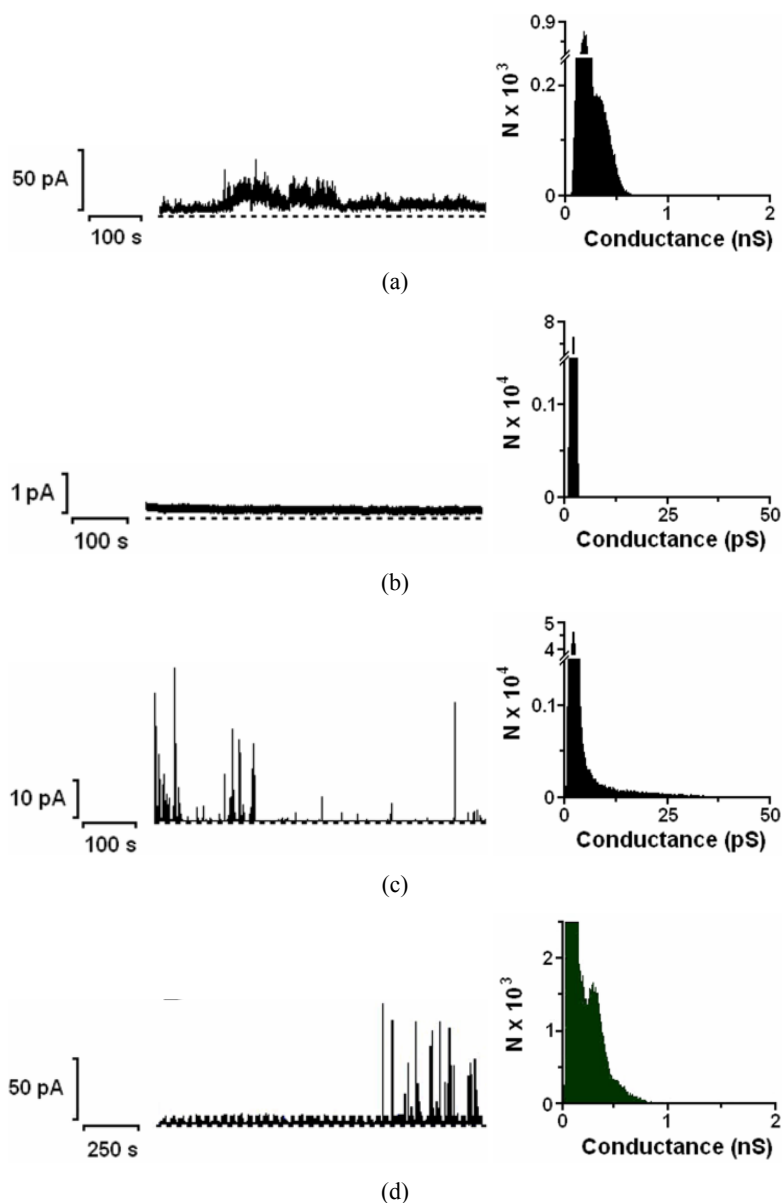
An important goal of ongoing research is to develop a fundamental understanding of how properties of the ENM and BLM affect their interactions. A strong influence of the BLM's lipid composition on ENM-induced pore formation has been demonstrated. Figure 2(a) shows the current through a pBLM as a function of time induced by carboxyl-functionalised QDs at a concentration of 0.6 $\mu\text{g/ml}$. The QDs induced integral conductance (a jump in current that continues for an extended period of time) through a 1,2-dioleoyl-*sn*-glycero-3-phosphocholine (DOPC) lipid bilayer at a potential of 50 mV, and increasing the potential to 100 mV led to rapid membrane disintegration. However, when the same QDs were introduced to a pBLM composed of a 3:1 ratio 1-palmitoyl-2-oleoyl-*sn*-glycero-3-phosphocholine (POPC) and 1-palmitoyl-2-oleoyl-*sn*-glycero-3-phosphoethanolamine (POPE) under identical conditions, no current was observed [Figure 2(b)]; a higher QD concentration (6 $\mu\text{g/ml}$) and higher voltage amplitude (100 mV) were necessary to induce current [Figure 2(c)]. A similar effect of lipid composition was also observed in experiments with carboxyl functionalised multi-wall nanotubes (FMWNT). Exposure to 10 $\mu\text{g/ml}$ FMWNT did not induce currents in a pBLM formed from a 3:1 ratio of POPC and POPE, even after increasing the FMWNT concentration to 100 $\mu\text{g/ml}$ [Figure 3(a)]. However, under the same conditions, pBLM formed from DOPC exhibited strong integral conductance at a FMWNT concentration of 10 $\mu\text{g/ml}$ [Figure 3(b)]. Currents induced by FMWNT at 100 mV increased with time

until the BLM ruptured [Figure 3(c)]. The trends observed in Figures 2 and 3 are consistent with the hypothesis that pBLMs having lower fluidity due to the use of lipids having a higher degree of saturation (POPC and POPE) are less susceptible to ENM-induced poration than pBLMs having higher fluidity due to the use of lipids with a lower degree of saturation (DOPC).

Planar BLM formed on standard electrophysiology cuvettes having an orifice about 150 to 250 μm in diameter exhibit low mechanical stability, exhibiting lifetimes on the order of an hour and rapidly breaking transmembrane potentials of 150 to 200 mV. However, pBLM formed on smaller orifices exhibit significantly higher stability (Hirano-Iwata et al., 2010a, 2010c). Sub-micron aperture sizes gave pBLMs that exhibited an order of magnitude longer lifetime and tolerated several times higher transmembrane potentials (Hirano-Iwata et al., 2010b; Han et al., 2007; Tiefenauer and Studer, 2008). A pBLM formed on a 100 nm nanopore milled through silicon nitride by focused ion beam had a minimum breakdown voltage of 250 mV (Kresak et al., 2009). Moreover, these nano-pBLM exhibited properties typical of conventional pBLM, as evidenced by patterns of pore formation by ion channel proteins and ionophores (Kresak et al., 2009; Studer et al., 2009). Im et al. (2010) reported a pBLM biosensor on a periodic nanopore array coupled with surface plasmon resonance (SPR) technique for SPR kinetic binding assays. The Worden lab has demonstrated that nano-pBLM can be used to measure ENM-membrane interactions. A pBLM formed across a 760 nm aperture drilled in silicon nitride showed gigaohm resistance by electrochemical impedance spectroscopy (EIS) and low transmembrane current when subjected to a constant potential of -80 mV [Figure 4(a)]. Then, ENM-induced pore formation was demonstrated for two types of ENM: PEG functionalised silica-core nanoparticles [Figure 4(b)] and FMWNT [Figure 4(c)]. Current traces following ENM addition showed the expected trends, including rapidly resealing current spikes and integral conductances similar to those observed in pBLM formed using conventional electrophysiology cuvettes.

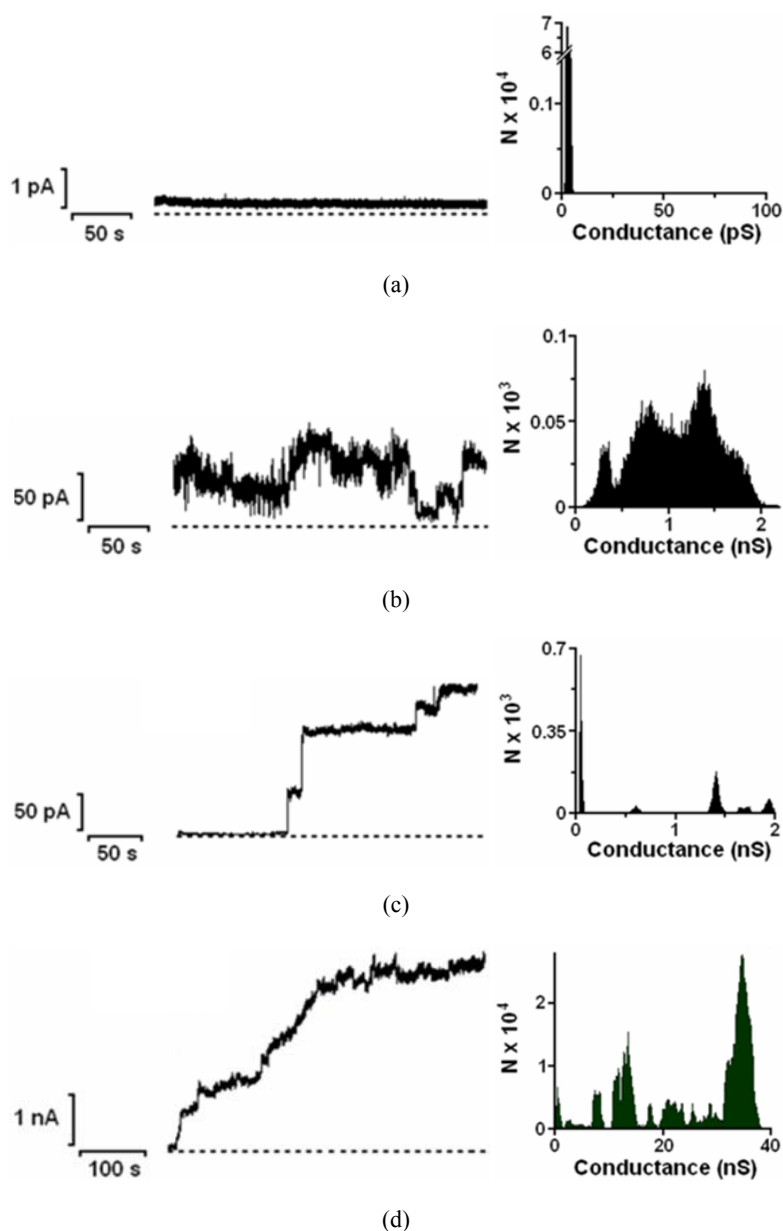
As a measure of the pBLM method's reproducibility, each experiment shown in Figures 2 and 3 involved at least five independent repetitions. Similar current profiles (e.g., integral current or rapidly resealing current spikes) were observed in about 80% of cases, but current amplitude varied between experiments, suggesting that ENMs induce defects in the membrane with variable pore size(s). To explore reproducibility of pBLM experiments between laboratories, similar experiments were conducted at both the Worden and Posner labs as part of the NIEHS-funded NanoGO consortium. In general, similar trends were observed in both labs. In the case of QDs, both labs observed rapidly resealing spikes as well as integral conductance, and conductance histograms for DOPC BLM for the two labs [Figures 2(a) and 2(d)] both showed a main peak that had a small shoulder at higher conductance. In the case of DOPC exposure to FMWNT at 100 mV, both labs observed integral conductance that increased with time, resulting in current histograms with multiple peaks associated with current jumps [Figures 3(c) and 3(d)]. However, differences in quantitative measures (e.g., time-averaged conductance) were observed between the two labs, likely due to differences in sensitivities and noise levels of the planar bilayer workstations in the two labs and subtle differences between experimental protocols.

Figure 2 Representative current traces (left) depicting ionic currents through BLM induced by QDs and the corresponding histograms of conductances (right), (a) A BLM formed using DOPC was exposed to 0.6 $\mu\text{g/ml}$ of QDs at a potential of 50 mV (b) A BLM formed using a 3:1 ratio POPC and POPE was exposed to 0.6 $\mu\text{g/ml}$ of QDs at a potential of 50 mV (c) A BLM formed using a 3:1 ratio POPC and POPE was exposed to 6.0 $\mu\text{g/ml}$ of QDs at a potential of 100 mV (d) A BLM formed using DOPC was exposed to 6.0 $\mu\text{g/ml}$ of QDs at a potential of 100 mV (see online version for colours)



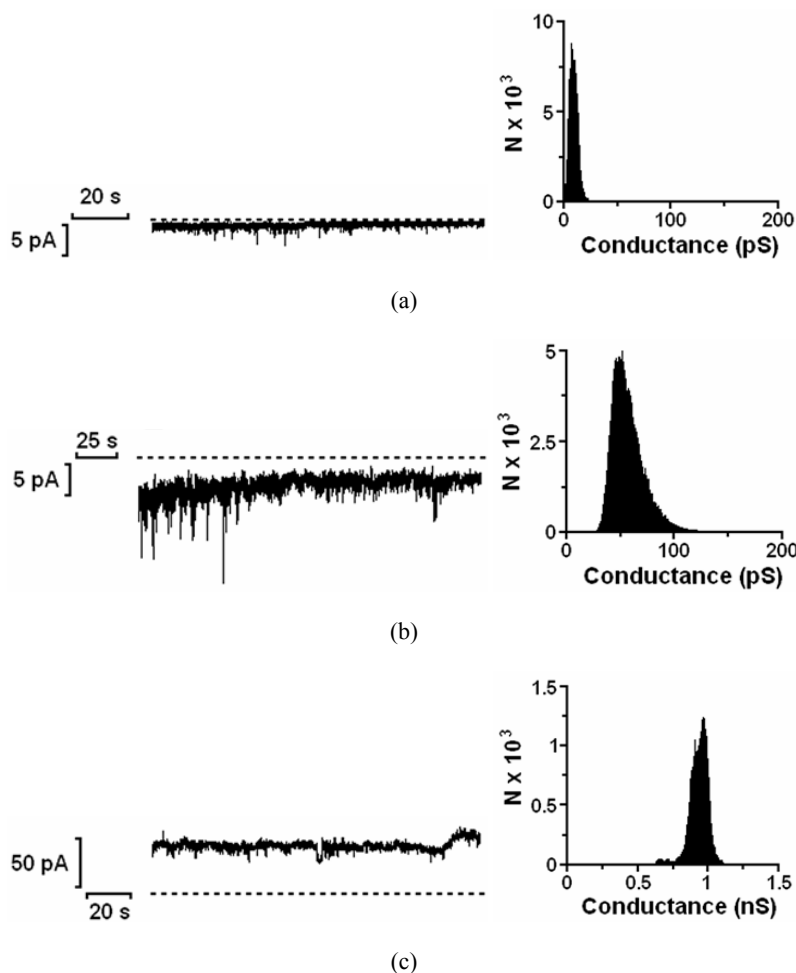
Notes: BLM were suspended between symmetric solutions of 20 mM KCl, 20 mM HEPES, pH 7.4. QDs were added to one side of the BLM. Dotted line shows zero current. Results in Figures 2(a) to 2(c) were obtained by the Worden group, and results in Figure 2(d) were obtained by the Posner group.

Figure 3 Representative current traces and histograms of conductances induced by FMWNT in BLM, (a) A BLM formed using a 3:1 ratio of POPC and POPE was exposed to 100 $\mu\text{g/ml}$ FMWNT at a potential of 50 mV (b) A BLM formed using DOPC was exposed to 10 $\mu\text{g/ml}$ of FMWNT at a potential of 50 mV (c) A BLM formed using DOPC was exposed to 10 $\mu\text{g/ml}$ of FMWNT at a potential of 100 mV (d) A BLM formed using DOPC was exposed to 6 $\mu\text{g/ml}$ of FMWNT at a potential of 100 mV (see online version for colours)



Notes: Conditions as in Figure 2. Dotted line shows zero current. Results in Figures 3(a) to 3(c) were obtained at MSU, and results in Figure 3(d) were obtained at ASU.

Figure 4 Ionic currents measured at room temperature for BLM formed across a 760 nm pore drilled in a silicon nitride window using a focused ion beam, (a) A BLM formed using a 3:1 ratio of POPC and POPE prior to the ENM exposure at a potential of -80 mV (b) A BLM formed using a 3:1 ratio of POPC and POPE was exposed to 300 $\mu\text{g/ml}$ of silica-core nanoparticles terminated with PEG oligomers at a potential of -80 mV (c) A DOPC BLM was exposed to 20 $\mu\text{g/ml}$ of FMWNT at a potential of 50 mV



Notes: The BLM was suspended between aqueous solutions of 20 mM KCl, 20 mM HEPES pH 7.4 . ENMs were added to one side of the BLM. Dotted line shows zero current.

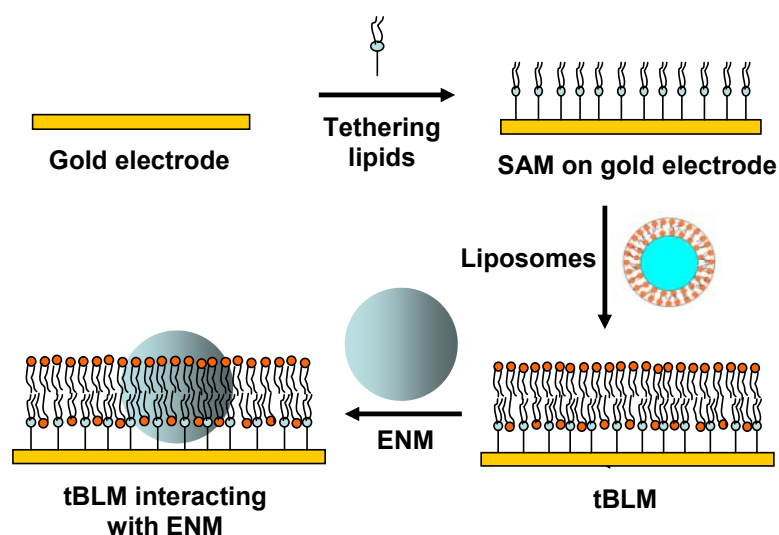
An important goal of ongoing research is to develop a fundamental understanding of how an ENM's properties influence pBLM current signatures. A variety of mathematical tools may be used to analyse the information-rich chronoamperometric current-*vs*-time profiles such as those shown in Figures 2 and 3. Quantitative measures commonly used to characterise pore formation by ion-channel proteins, including histograms, average conductance values, and number of conductance events greater than a threshold value, are also useful to characterise ENM-BLM interactions. Using these tools, qualitative differences BLM-disruption patterns have been noted. Early work has suggested that

spherical nanoparticles often trigger current spikes, presumably caused by individual pores opening and then rapidly closing. On the other hand, high-aspect ratio ENMs (e.g., FMWNT) often induce integral conductance that fluctuates in magnitude, suggesting formation of pores having greater stability, perhaps due to penetration of the bilayer by the ENM, as is illustrated in Figure 1. The significance of these trends from the standpoint of nanotoxicity is not yet clear, and the quantitative measures that best characterise an ENM's potency at BLM disruption have not yet been identified.

2.2 Tethered bilayer lipid membrane

Immobilisation of BLM on surfaces offers advantages over pBLM, including enhanced stability. Supported BLM can be self-assembled directly on hydrophilic surfaces (Nollert et al., 1995). However, this approach lacks an ion reservoir on both sides of the BLM needed to measure transmembrane ion flux. This deficiency can be overcome using the tethered bilayer lipid membrane (tBLM) platform (Krishna et al., 2003), in which some of the phospholipids composing the lower leaflet are chemically tethered to the underlying electrode (Rossi and Chopineau, 2007). Figure 5 shows the process of tBLM formation (adapted from Jadhav et al., 2008). The headgroups of tethering lipids are commonly terminated with thiol or disulfide groups that form thiol linkages to gold (Atanasov et al., 2006; Prime and Whitesides, 1991). An advantage of depositing tBLM on gold is that a variety of sensitive surface-characterisation techniques, such as quartz crystal microbalance with dissipation, SPR, atomic force microscopy (AFM), and ellipsometry, can be applied (García-Sáez and Schwille, 2010; Hook et al., 2008). High-impedance tBLM have also been formed on hydrogel-coated indium-tin oxide electrodes (Kibrom et al., 2011).

Figure 5 Process of forming tethered BLM on a gold electrode (see online version for colours)



Notes: A self-assembled monolayer is first formed on a gold electrode. Then, liposomes are deposited and ruptured to form the top leaflet of the tBLM. The tBLM can then be exposed to pore-forming agents, such as gramicidin (Jadhav et al., 2008) or ENM.

Cyclic voltammetry (CV) and EIS can sensitively measure ion migration through pores formed in tBLM by ENMs, ionophores, channel-forming proteins, etc. In EIS, the tBLM is subjected to a transient electrical potential consisting of a constant DC component superimposed on an AC component that varies in frequency. The resulting impedance data are analysed using an equivalent-circuit model to calculate the tBLM's membrane resistance (R_m). Alternatively, finite element analysis can be applied to analyse EIS spectra in terms of defects in the tBLM that range from small pinholes to large membrane-free patches (Kwak et al., 2010). Use of these quantitative approaches allows drops in R_m to be calculated following exposure to pore-forming agents, such as the peptide gramicidin and the ionophore valinomycin (Kohli et al., 2006; Jadhav et al., 2008). Gramicidin is selective for monovalent ions (Hladky and Haydon, 1972), while valinomycin is selective only for potassium ion (Kohli et al., 2006; Raguse et al., 1998), providing a means to validate proper functional behaviour of tBLM.

In recent years, the tBLM platform has been characterised and validated for a variety of biomembrane research (Jadhav et al., 2008, 2012; Adams et al., 2003; Oh et al., 2008; Robertson et al., 2008; Terrettaz et al., 2003; Tun and Jenkins, 2010; Jadhav and Worden, 2008). The tBLM system has recently been adapted to characterise interactions of ENMs with biomembranes. Exposure of a DOPC tBLM to functionalised silica core nanoparticles gave a time-dependent decrease in R_m . Statistical analysis confirmed that the method could distinguish between silica-core ENMs that were identical except for the surface functional group. While the mechanism of ENM-induced changes in R_m has not been studied, AFM studies have documented hole formation and/or expansion of existing defects in supported BLM following exposure to polyamidoaminodendrimers (Mecke et al., 2004), cationic nanoparticles (Leroueil et al., 2008) and polycationic polymers (Mecke et al., 2005). Molecular dynamics (MD) simulations have provided additional insight into the pore formation mechanism (Lee and Larson, 2006, 2008, 2009).

2.3 Outlook for high-throughput applications of pBLM and tBLM

The classical pBLM method, while sensitive and powerful, has disadvantages that limit its practicality for ENM screening. The method is slow, tedious, requires a skilled technician, and, due to variability between runs, requires multiple replicates ($n > 5$ often). The tBLM method (Figure 5) does not require manual procedures, as the solutions containing the tethering lipids and then liposomes can be automatically delivered to the electrodes via pumps. However, the incubation times typically used for self-assembly of the tethering layer and upper leaflet are on the order of hours. Higher throughput can be achieved in several ways:

- 1 by accelerating the BLM-assembly process
- 2 by accelerating the data-acquisition phase, in which the BLM disruption by the ENMs is measured
- 3 by running multiple assays in parallel
- 4 by operating the system more hours per day.

Array architectures supporting parallel assays, such as a robotically controlled multi-well plate system (Aftab and Hait, 1990), are ideal for high-throughput applications.

Although array structures for BLM studies are still in their infancy, arrays have been shown to greatly enhance the efficiency of analysis by forming multiple BLMs simultaneously (Im et al., 2010; Baaken et al., 2011; Thei et al., 2010; Zagnoni, 2012; Studer et al., 2009). The pBLMs can be formed in an automated fashion by flowing lipid-containing solvents through microfluidic channels on both sides of a nanopore film (Malmstadt et al., 2006; Osaki et al., 2009, 2011; Suzuki et al., 2007; White et al., 2007; Zagnoni et al., 2009; Hirano-Iwata et al., 2012). Thus, forming arrays of multiple BLM with different functionalities using multi-channel microfluidic networks appears feasible. Additional gains in throughput could be obtained by integrating electrochemical instrumentation onto microelectronics chips (Genov et al., 2006; Gore et al., 2006; Yang et al., 2009a) including those used for EIS (Manickam et al., 2010; Min and Parve, 2007; Yang and Mason, 2009; Yang et al., 2009b). Electrode and sensor arrays have been formed on the surface of microelectronic chips (Eversmann et al., 2003; Schienle et al., 2004; Yue et al., 2008; Yun et al., 2000; Zhu and Ahn, 2006). These microelectronics electrochemical instrumentation chips reduce noise, providing higher accuracy and eliminating the need for bulky bench-top instruments.

3 Liposome leakage assay

Some of the challenges associated with electrical measurements can be addressed by using optical assays that measure dye leakage from liposomes. Liposomes are artificially prepared vesicles composed of a lipid bilayer shell with an aqueous interior. For more than 30 years, liposomes have served as a research platform to study lipid bilayers. Liposomes have been used for quantifying lipid bilayer leakage induced by lipid lytic compounds (Bechinger, 1997; Chatterjee and Banerjee, 2002; Gervais et al., 2011; Herbig et al., 2006; Matsuzaki et al., 1997; Tosteson and Tosteson, 1981). Measurements are typically performed by loading the liposomes with self-quenching fluorescent dye at a concentration high enough (> 50 mM) to quench fluorescence. When membrane-disrupting compounds or nanoparticles are added to the solution, dye escapes from the liposome, reducing quenching and increasing fluorescence, which can be measured with fluorescence spectroscopy (Moghadam et al., 2012; Ralston et al., 1981). The specificity, homogeneity, and availability of large-batch production of liposomes has encouraged their use in robust high-throughput screening assays (Chatterjee and Banerjee, 2002; Gervais et al., 2011). The approach can provide insight into the disruptive mechanisms, e.g., permeabilisation of lipid bilayers and pore formation, by modulating the osmotic pressure across the liposome and by working near the phase transition temperature (Benachir and Laflour, 1995; Rex and Schwarz, 1998).

Liposome leakage from ENMs has been shown to correlate well with *in vitro* cell studies. Goodman et al. compared the cellular toxicity of 2 nm gold nanoparticles with liposome leakage assays. They showed that cationic particles are moderately toxic and that anionic particles are non-toxic; these results correlated well with the lytic effects on L- α -stearoyl-oleoyl-phosphatidylcholine (SOPC) and L- α -stearoyl-oleoyl-phosphatidylserine (SOPS) lipid bilayer vesicle-disruption assays (Goodman et al., 2004).

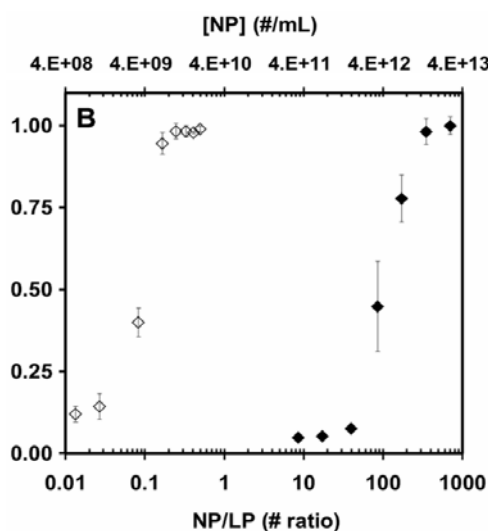
Multi-lamellar vesicles (MLV) typically exhibit considerable heterogeneity in size and contain many internal compartments, which make them more resistant to defects and

disruption than uni-lamellar vesicles (UV). Consequently, UV are better suited for studying liposome permeability and fusion than are MLV (Hope et al., 1986; Mayer et al., 1986; Sila et al., 1986). Large uni-lamellar vesicles (LUVs) are relatively homogeneous in size, contain relatively large volumes (resulting in higher assay signal to noise ratios and more closely resemble the structure of cell membranes (MacDonald et al., 1991). The use of LUVs helps assure that the nanoparticles interact with a single lipid bilayer.

Liposome-leakage assays can be used to detect ENM-induced disruption of lipid bilayers. Hirano et al. studied the effect of single-walled carbon nanotubes (SWNTs) conjugated with positively charged lysozymes (LSZ) on the leakage of negatively charged 200 nm UVs composed of 1,2-dioleoyl-sn-glycero-3-phosphoglycerol (DOPG)/DOPC. They reported similar leakage caused by SWNTs-LSZ conjugates and LSZ amyloid fibrils, while only marginal leakage occurred for bare SWNT's (Hirano et al., 2010). Posner's group have investigated the role of surface functionality and charge of 10 nm gold and titanium dioxide (TiO₂) nanoparticles on the disruption of DOPC LUVs (~100 nm) using dye-leakage assay. They used polydiallyldimethylammonium chloride (polyDADMAC), tannic acid, polyvinylpyrrolidone (PVP) (NanoComposix, San Diego, CA), and sodium polyacrylate functionalised particles to elucidate the role of ENM concentration and surface charge on the kinetic rate and steady-state leakage rate of liposomes. Our work showed that ENMs induce leakage that increases exponentially and reaches a steady state value after several hours. Figure 6 shows the steady state leakage induced by polyDADMAC functionalised 10 nm Au ENM(+) and a well-known lytic, melittin peptide, as function of number density and number of particles per liposome (Moghadam et al., 2012). Both Au(+) ENMs and melittin induce leakage that increases with concentration following a sigmoidal shape. A variety of chemical systems exhibit sigmoidal responses as a function of a concentration, including cooperative ligand binding and dissociation (Juska, 2008), pH titration, and the dose-response curve in toxicity studies.

Leakage from liposomes was detected for nanoparticle concentrations as low as 20 ppb mass. These measurements suggest ENMs trigger leakage similar to melittin and that a single Au(+) nanoparticle may induce measurable leakage from a liposome (relative to ~300 molecules for melittin) (Benachir and Lafleur, 1995). Figure 7 reports the effects of surface coating and particle charge on the steady-state liposome leakage by TiO₂ or Au ENMs at mass concentration ratios of 0.01 (i.e., 60 ppb mass of nanoparticle and 6 ppm mass of lipid). These results show that leakage is a strong function of surface charge with Au(+) ENMs inducing 94% of leakage and only marginal leakage measured for tannic acid and PVP coated Au and TiO₂ ENMs. Low leakage induced by negatively charged ENMs was attributed to electrostatic repulsion by negatively charged liposomes. A prior study showed that SWNTs coated with positively charged proteins caused the leakage of negatively charged liposomes, while uncoated SWNTs had a minimal effect (Hirano et al., 2010). Their results also showed minimal leakage induced by negatively charged ENMs in a good agreement with our observations. Hou et al.'s (2012) work on adsorption of ENMs to lipid bilayers also suggests that the electrostatic interactions largely control non-specific binding of ENMs to a bilayer surface. Collectively, the finding suggests that an ENM's surface coating, which determines the surface charge, plays a key role in the interaction of metallic and metal oxide nanoparticles with DOPC lipid bilayer vesicles, and changing the core composition has an insignificant effect.

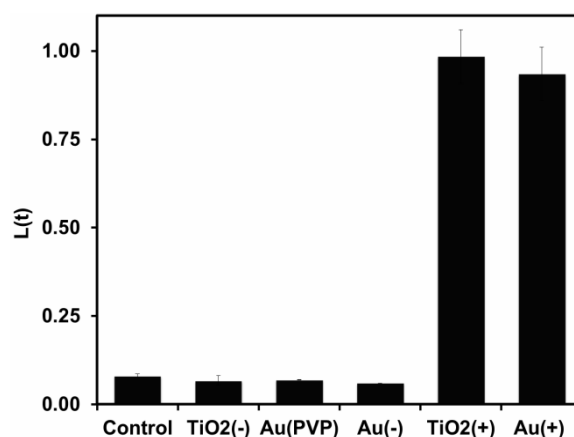
Figure 6 Comparison of liposome leakage induced by 10 nm positively charged Au nanoparticles (Au ENM (+)) (\diamond), versus melittin (\blacklozenge) as a function of (B) number concentrations (top axis), or particle number ratio (lower axis) of Au ENM(+) or melittin to liposome after reaching a steady state leakage at pH = 7.4 (20 mM HEPES)



Notes: The error bars indicate \pm one standard deviation.

Source: Reprinted with permission from Moghadam et al. (2012)

Figure 7 Comparison of fraction of liposome leakage $L(t)$ induced by 10 nm nanoparticles with different surface coating, charge characteristics, and core compositions, indicating the percent leakage induced by negatively charged TiO₂ nanoparticles (TiO₂(-) ENM), positively charged TiO₂ nanoparticles (TiO₂(+) ENM), negatively charged Au nanoparticles (Au(-) ENM), positively charged Au nanoparticles (Au(+) ENM), as well as polyvinylpyrrolidone coated Au nanoparticles (PVP Au ENMs) at pH = 7.4 (20 mM HEPES)



Notes: The percent leakage was recorded after 6 h of interactions. The nanoparticle mass concentrations were 60 $\mu\text{g/L}$ and lipid concentration was 7.83 μM . The error bars indicate \pm one standard deviation.

Source: Reprinted with permission from Moghadam et al. (2012)

Several studies have suggested that electrostatic interactions governed by surface functionality (e.g., positive particles with negatively charged lipids) are critical to mediating leakage. To evaluate whether molecules used to coat ENMs caused liposome leakage on their own (without the ENM), researchers compared the leakage induced by DADMAC Au(+)ENMs with the Au(+)ENMs filtrate (potentially containing free DADMAC) and free DADMAC solution freshly prepared. They observed insignificant leakage by DADMAC solution, filtrate, or control relative to the Au(+)ENMs. This finding indicates that the DADMAC does not induce leakage on its own and must associate with nanoparticles to cause liposome leakage. The result is consistent with previous work indicating that cationic LSZ do not permeabilise liposomes unless associated with a tubular nanostructure (i.e., SWNT) (Hirano et al., 2010).

The large number of particle physicochemical characteristics, lipid compositions, and electrolyte conditions necessitate the use of high-throughput methods. Liposome leakage assays have been conducted in high-throughput using microtiter plates (Hadjicharalambous et al., 2008; Kichler et al., 1997; Kusonwiriawong et al., 2003). Extending ENM liposome leakage assays to a high-throughput format would leverage the robotics infrastructure that has been widely used in the biotechnology industry.

4 ENM adsorption to lipid bilayers

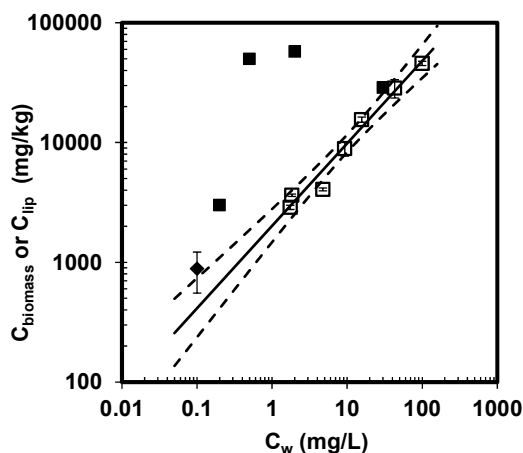
Quantitative approaches for predicting toxicity and bioaccumulation of ENMs can be developed that account for the collective influence of ENM properties on lipid membrane-water distribution (K_{lipw}). For chemicals that distribute between different organic phases, both octanol and water distribution coefficients (K_{ow}) and K_{lipw} are influenced by single or multiple parameters of organic pollutants, such as molar volume, aqueous solubility, and acidity constants (Chiou et al., 1982; Jafvert et al., 1990). Global descriptors like K_{ow} are widely used for predictive toxicology and bioaccumulation of organic pollutants (Chiou et al., 1977; Neely et al., 1974) and are incorporated into current US EPA models (ECOSAR, Oncologic). Analogous empirical global descriptor methods to partitioning have begun to be employed for ENMs (Petersen et al., 2010; Jafvert and Kulkarni, 2008; Giri et al., 2009; Hristovski et al., 2011; Wang et al., 2010). K_{ow} recently was determined for carbon nanotubes (Petersen et al., 2010), C_{60} (Jafvert and Kulkarni, 2008), dendrimers (Giri et al., 2009), as well as metals and metal oxides (Hristovski et al., 2011), but the validity of K_{ow} as an appropriate descriptor for some ENMs is under some scrutiny (Giri et al., 2009; Hristovski et al., 2011; Petersen et al., 2010). The Posner group and others have observed that in octanol-water systems, ENMs can accumulate at interfaces and form emulsions (Giri et al., 2009; Binks and Rodrigues, 2005; Hristovski et al., 2011) that complicate the design, quantification, and interpretation of K_{ow} experiments and thus their use in predictive models.

Synthetic BLM have been used increasingly as replacements for octanol in partitioning studies with organic pollutants. The lipid bilayer-water distribution coefficient (K_{lipw}) has been shown to be a more appropriate descriptor than K_{ow} for the biological membrane uptake of some classes of hydrophobic (Dulfer and Govers, 1995; Kwon et al., 2006; Opperhuizen et al., 1988) and ionisable organic pollutants (Escher and Schwarzenbach, 1996), as well as surfactants (Muller et al., 1999). A BLM's mass is nearly all at the interface and can be quantified. This eliminates the difficulty encountered

in the octanol-water partitioning of surface-active compounds and potentially some types of ENMs that may also accumulate at the octanol-water interface (Binks and Rodrigues, 2005; Giri et al., 2009; Hristovski et al., 2011).

To evaluate the lipid bilayer-water distribution for ENMs, Hou et al. (2011, 2012) have developed a robust approach using lipid bilayers-non-covalently-supported on silica spheres, which are commercially available as TRANSILTM binding kits. Hou et al. (2011) has examined the lipid bilayer-water distribution of fullerene C_{60} and functionalised polyhydroxylated C_{60} fullerol ($C_{60}(ONa)_x(OH)_y$, $x + y = 24$) nanomaterials. Their results indicate that the fullerene nanomaterials achieve a steady state distribution in 24 h, and the fullerene distribution between the aqueous phase and lipid bilayers appears non-linear across two orders of magnitude in aqueous fullerene concentrations. The lipid bilayer-water distributions of both C_{60} and fullerol/nano-aggregates are pH-dependent with accumulation in lipid bilayers increasing systematically as pH decreased from 8.6 (natural water pH) to 3 (the low end of physiologically relevant pH). This pH dependency, which we control using buffered solutions, modulates the zeta potentials of the fullerene nanomaterials and leads to similar patterns as previously observed for the lipid bilayer-water distribution behaviour of ionisable organic pollutants. The lipid bilayer-water distribution coefficient (K_{lipw}) for C_{60} was larger than that of fullerol at a given pH, indicating greater propensity for C_{60} aggregates to interact with lipid bilayers.

Figure 8 Preliminary comparison of lipid bilayer-water distribution of C_{60} aggregates (nC_{60}) measured at pH = 7.4 from this study with existing bioaccumulation studies of nC_{60} under similar solution chemistry



Notes: The organism (water flea, *Daphnia magna*)-water distribution bioaccumulation data (\square $C_{biomass}$ versus C_w) from this report is plotted along with a solid line representing the fitted Freundlich isotherm. $C_{biomass}$ is the mass of nC_{60} accumulated in daphnia normalised by daphnia biomass (i.e., mg nC_{60} /kg biomass) based on dry weight (\blacksquare), or lipid content (\blacklozenge). Dashed lines indicate 95% confidence interval.

Source: Bioaccumulation data are from Oberdorster et al. (2006), Tao et al. (2009) and Tervonen et al. (2010) with all studies using *Daphnia magna* as test organisms; Reprinted with permission from Hou et al. (2011)

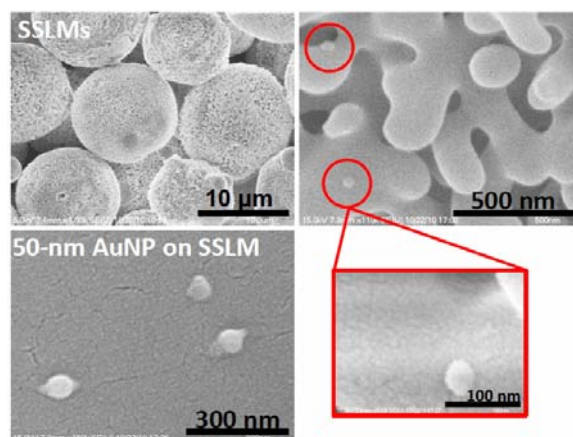
Hou et al. assessed the utility of lipid bilayer-water distribution in prediction of bioaccumulation in aquatic organisms by comparing their data with existing aquatic organism bioaccumulation studies for C₆₀ nano-aggregates as shown in Figure 8. Bioaccumulation is important in that if a chemical tends to reside in organisms it is likely to exert long-term biological effects such as food-chain transfer. Therefore, bioaccumulation potential is an important aspect in quantifying ecological risks. Figure 8 shows a preliminary comparison of the lipid bilayer-water distribution of nC₆₀ at pH = 7.4 from Hou's study with existing bioaccumulation studies using *Daphnia magna* (i.e., water flea) at pH = ~7 (Oberdorster et al., 2006; Tao et al., 2009; Tervonen et al., 2010). Bioconcentration factor (BCF), defined as chemical concentration measured in biota divided by chemical concentration measured in water, traditionally has been used to assess the bioaccumulation potential of chemicals. The reported or estimated log BCF ranges are 2.98–4.40 (dry biomass-based) and 3.67–4.16 (lipid content-based). The daphnia-water distribution trend is qualitatively consistent with the lipid-water distribution data. Tao et al. (2009) reported that nC₆₀ accumulated in biomass well correlated to the lipid content. The single estimated lipid-based log BCF of 3.67–4.16 from Tao et al. compares well to our log K_{lipw} of 3.62 at similar exposure concentration.

Recent studies have begun to examine the role of ENMs' physicochemical properties in their interactions with biomembranes and cellular uptake. Selection of meaningful dosimetry (e.g., mass, surface area, or particle number concentration) can aid in the understanding of nano-bio interactions. There is a lack of consensus on the appropriate dosimetry for nanomaterials. The behaviour of ENMs in the aqueous phase is dynamic because they can aggregate, settle, diffuse, or interact with biological surfaces depending on their physicochemical properties, such as size distribution, surface charge, and functionality, as well as the dependence of these properties on the solution chemistry (Teeguarden et al., 2007). These dynamic processes relate specifically to the number density and size distribution of nanoparticles rather than their mass concentrations. The analogy for dissolved molecular chemicals would be a comparison of doses for two compounds using molar units rather than mass units. Applying to nanoparticles the dose metric for molecular solutes based on mass concentration can yield different interpretations of the response endpoints. For example, for a given mass concentration of the same nanoparticles with different sizes, the corresponding particle number or surface area concentration can be larger by orders of magnitude for the smaller diameters.

Hou et al. also explored the dosimetric selection on the distribution of gold nanoparticles (Au NPs) to lipid bilayers (Hou et al., 2012). Using tannic acid functionalised Au NP from 5 to 100 nm, they found that typically 10–60% of Au NP mass concentration from the aqueous phase distribute to lipid bilayer, but only cover < 2% of lipid bilayer surface as supported by the SEM images in Figure 9. These results show that smaller sized Au NPs accumulate more rapidly to lipid bilayers than do larger ones. Large Au NPs distribute to lipid bilayer to a greater extent on mass basis than small Au NPs, but the trend reverses on particle number density basis. The faster accumulation to lipid bilayers for small nanoparticles can be qualitatively rationalised by the Smoluchowski collision rate equations and the classical colloid theory [i.e., Derjaguin-Landau-Verwey-Overbeek (DLVO) theory]. The Smoluchowski equations state that the initial collision rate increases with greater number density consistent with the larger number density for small Au NPs in a given Au mass concentration (Elimelech et al., 1998). Hou's analysis suggests that number concentration, along with Au NP diameter, may be the more appropriate dosimetric parameter for mechanistically describing the

nano-bio interaction. Across the various Au NP sizes, they measure the lipid bilayer-water distribution coefficient ($K_{lipw} = C_{lip} / C_w$) as 450 L/kg lipid, which is independent of dosimetric units. The K_{lipw} value may be used to predict the affinity of spherical Au NPs across a certain size range toward lipid membranes.

Figure 9 SEM images of 50-nm tannic acid coated Au NP adsorbed onto solid-supported lipid membranes (see online version for colours)



Source: Reprinted with permission from Hou et al. (2012)

Overall, Hou's studies suggest that lipid bilayer-water distribution is a promising predictor for accumulation of ENMs in lipid bilayers specifically (Figure 1) and potentially bioaccumulation in aquatic organisms. Because lipid bilayers are simpler and easier to manipulate than organisms, measurement of ENM adsorption to lipid bilayers has the potential to be conducted in high throughput, such as in microtiter plates, to screen ENMs for bioaccumulation and toxicity potentials.

5 Theoretical modelling of ENM interactions with lipid bilayers

AFM provides clear images of the formation of holes in supported DMPC bilayers by generation seven (G7) amine terminated dendrimers, but not by lower order dendrimers or by G7 PAMAM dendrimers terminated by acetamide end groups (Mecke et al., 2005; Leroueil et al., 2007). Cationic amine-terminated dendrimers have a favorable attraction to the lipid head groups, and the observed chemical and size effects observed were explained based on a balance of surface energy and head group packing constraints, where smaller dendrimers lead to more difficulty in optimising both the inner and outer lipid monolayer head-group packing densities. The strongly disruptive effect of cationic ENMs is due to their attraction to the overall negative charge that is typical of mammalian cell membranes. MD simulations using a CHARMM potential, implicit solvent, and a Langevin noise term support the concept that highly charged cationic dendrimers are strongly attracted to the BLM, though computational limitations restricted the calculations to G3 dendrimers (Kelly et al., 2008).

This work stimulated a series of MD simulations of the effects of various ENMs on BLM using all-atom and coarse-grained descriptions (Muller et al., 2006; Deserno,

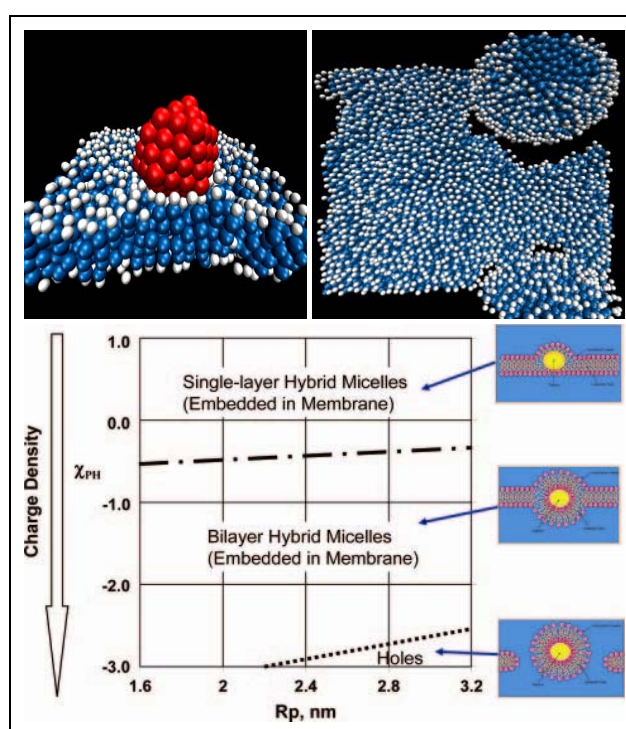
2009). Three of the most commonly used coarse-grained models are a united atom model developed by the Klein group (Shelley et al., 2001; Shinoda et al., 2010), the Cooke model (Cooke et al., 2005; Deserno, 2009) that uses pair potentials with broad minima and the MARTINI model (Marrink et al., 2004, 2007) that typically condenses four heavy atoms to one bead, and uses a coarse-grained solvent. The non-bonded interactions in the MARTINI model are Lennard-Jones and Coulomb, while the bonded interactions are harmonic bond-stretching and bond-bending. A basic requirement of the coarse-grained models is that they reproduce the liquid-like structure of lipids, which overcomes problems with simple Lennard-Jones models that have difficulty reproducing the correct BLM liquid structures. Studies of membrane disruption due to PAMAM dendrimers using the MARTINI force field support the earlier conclusions (Lee and Larson, 2008) and also show that cationic linear polymers also disrupt BLM. However cationic dendrimers of larger size have a stronger effect on BLM, while the effect of cationic linear polymers on BLM appears to saturate at larger size. Cation-coated AuNP-BLM response analysed (Lin et al., 2010) using MD simulations with the coarse-grained MARTINI force field (Marrink et al., 2004), indicates that nanoparticles with diameter approximately 2.2 nm produce hydrophilic pores allowing water translocation, and that membrane disruption is stronger for ENMs with higher concentrations of cationic headgroups. Both atomistic and coarse-grained MD simulations demonstrate that small hydrophobic carbon nanoparticles, including various fullerenes (Wong-Ekkabut et al., 2008; Monticelli et al., 2009; Jusufi et al., 2011), nanotubes (Monticelli et al., 2009), and graphene flakes (Titov et al., 2010) segregate to the hydrophobic core of lipid membranes; moreover suitable end functionalisation can stabilise transmembrane nanotube configurations (Dutt et al., 2011), which are candidates for artificial drug-delivery channels. Nanoparticle translocation is a key goal for applications to drug delivery, and mechanisms for translocation include diffusion, pore formation, and endocytosis.

These insights and those garnered from studies of cationic ENMs have been extended to a more complete analysis of the dependence of ENM translocation mechanisms on ENM size, shape and surface functionalisation (Yang and Ma, 2010; van Lehn and Alexander-Katz, 2011), with smaller particles of lower charge being more diffusive and larger cationic particles favouring disruptive pore formation. Thermodynamic models provide a broader perspective of the stable and metastable phases of BLM-ENM systems. Mechanical models that balance the ENM-membrane interaction energy against the energy cost of bending the BLM, where the bending modulus is typically $20k_B T$ (Helfrich, 1973; Gao et al., 2005), provide a first estimate of the equilibrium states. The phase diagram of ENM-BLM systems as a function of ENM size and charge has been calculated using a self-consistent field theory method (Ginzburg and Balijepalli, 2007).

The results are reproduced in Figure 10, along with images of MD simulations using similar parameters within the Cooke coarse-grained model, for nanoparticles that are strongly attracted to the lipid heads (Cooke et al., 2005). In both cases, there is a change in morphology as a function of the nanoparticle size, from an intact ENM/BLM morphology at small nanoparticle size to a ruptured morphology at larger nanoparticle size. The onset of poration is tuned via the interaction strength between the ENM and the BLM. Figure 10 illustrates a case where an ENM of radius 4.4 nm causes poration while an ENM of radius 2.7 nm does not. The morphologies are, however, different for the smaller ENM sizes, with the MD simulations suggesting that the ENMs remain bound to the outer surface of the BLM, while the self-consistent field theory suggests that the

nanoparticle forms a stable complex on the interior of the bilayer. Further simulations are required to test the stability of the structure suggested by the self-consistent field theory. Because the self-consistent theory is two dimensional, the nanoparticles in the theory are actually rods. The nanoparticle sizes treated within both theories and in all of the simulations discussed above are relatively small (at most a few nanometres), due to computational constraints. In contrast many experiments use nanoparticles in the size range 10–200 nm, which is extremely challenging for even the most coarse-grained MD models currently available.

Figure 10 Coarse grained MD NP/lipid morphologies (top two figures) found using the Cooke model (see online version for colours)



Notes: A small hydrophilic NP (left) does not rupture the bilayer while a larger hydrophilic NP (right) is covered by lipid to form a NP-lipid liposome and leading to poration. Phase diagram of NP-lipid systems within self-consistent field theory (Ginzburg and Balijepalli, 2007).

In summary, simulation studies are consistent with the experimental observations, predicting that larger cationic ENMs are disruptive to BLM, and that small hydrophobic ENMs aggregate to the core of BLM. Further developments in multi-scale modelling are required to simulate larger ENMs interacting with lipid membranes and to capture dynamical processes at the larger time scales that are relevant to high throughput ENM screening methods. Simulations are also being used to search for ENM size, shape and charge combinations that enable efficient NP translocation with minimal disruption to the BLM, as is required for applications to drug-delivery systems.

6 Summary and outlook

This paper has reviewed four assay platforms to measure molecular interactions between ENMs and synthetic BLM. These *ex-vivo* assays offer advantages over traditional *in-vivo* and *in-vitro* toxicity assays, including

- 1 the composition of the BLM can be precisely controlled
- 2 the assays are customisable via selecting components included in the BLM
- 3 experiments can be performed under a wider range of conditions than is possible using living systems
- 4 the assays are readily adaptable to high-throughput operation
- 5 theoretical models that predict molecular interactions between ENMs and BLM may be used to interpret the results.

Each of the platforms offers distinct advantages. The electrochemical methods measure transmembrane ion flux, which is important for both cell viability and intercellular signalling. The pBLM method leverages well established electrophysiology tools to characterise ENM-induced membrane perturbations with single-pore sensitivity, whereas the tBLM method is more robust and uses less expensive equipment. High-throughput can be achieved for both electrochemical methods via integration of microfluidics and microsystem array architectures. The liposome-leakage platform use sensitive optical methods to measure the fluorescence increase as self-quenching fluorescent dyes escape LUV under the influence of membrane-disrupting ENM. This approach has been validated for multiple types of ENM, and results have been correlated with *in-vitro* cell toxicity studies. The platform based on ENM adsorption to lipid bilayers offers advantages over octanol-water partitioning for measuring bioaccumulation, because lipid bilayers are a more biologically relevant model reservoir. The use of commercially available, BLM-coated silica spheres facilitates standardisation. Ongoing research is clarifying the role of particle size on dose response relationships. Both the liposome-leakage and ENM-adsorption assays can be performed in high-throughput mode using multi-well optical plate readers.

Because all of four approaches are based on molecular interactions between ENMs and BLMs, the assay results are sensitive to the solution chemistry. For example, the ionic strength inside and outside of the liposomes must be relatively well matched, or the osmotic pressure can deform and destabilise the membrane. In the electrochemical methods, the ionic strength must be sufficient to conduct current and obtain a reasonable signal to noise ratio but not so high as to induce ENM aggregation. Thus, electrolyte composition and concentration must be considered into context of both dispersion stability and biological relevance. In general, BLM-based assays can be performed at much lower electrolyte concentrations than is possible in *in-vivo* and *in-vitro* assays, which often suffer from ENM aggregation.

Some common trends have already emerged from the BLM-based platforms. Positively charged ENMs uniformly induced more disruption to bilayers for both pBLM and liposome-based systems. In addition, pBLMs formed from lipids whose tails are more saturated (POPC and POPE) are less susceptible to ENM-induced poration than pBLMs formed using lipids whose tails are less saturated (DOPC). We also found that

results on pBLM systems could be reproduced in different labs with similar but unique experimental systems. This finding is important, because the high variability seen in *in-vivo* and *in-vitro* assay platforms has motivated extensive investigation by the NIEHS NanoGO programme. Overall, the BLM-based assays that were originally developed to study ion channel proteins, toxins, and other agents that disrupt cell membranes appear to be useful for ENM when proper consideration is given to key factors including electrolyte composition and pH.

Additional research is needed to correlate results of these emerging BLM-based assays with traditional *in-vitro* and *in-vivo* toxicity assays. As the BLM-based assay protocols are further refined and validated, they can be readily extended to investigate the effect of other ENM-related molecular phenomena on toxicity. For example, under physiological conditions, ENM interact with a variety of biomolecules, including proteins (Lynch et al., 2007). Formation of a protein-containing corona on ENM can influence the ENM's surface properties and thus its tendencies to aggregate and interact with cell membranes (Lynch et al., 2009). The integration of multiple assay platforms to measure ENM-BLM interactions with fundamental knowledge of corona-formation dynamics (Lundqvist et al., 2008; Cedervall et al., 2007) would enable high-throughput assays of ENM-BLM interactions to be conducted under increasingly more physiologically relevant conditions, and would improve correlations between these assays and traditional *in-vitro* and *in-vivo* toxicity assays. Development of correlations between the various assay platforms would provide a broader database for developing improved risk-assessment models, enable high-throughput methods to screen ENM libraries for toxicity potential, and facilitate *in-silico* design of ENMs that meet desired performance criteria as well as safety standards.

Acknowledgements

Financial support was provided by the National Institute of Environmental Health Sciences under award RC2 ES018756, the U.S. Department of Energy under award DE-FG02-08ER64613 with Daniel Drell as programme manager, the National Science Foundation under grants CBET-0932885 and CBET-0756703, and Semiconductor Research Corporation, under Task No. 425.025.

References

- Adams, M.L., Enzelberger, M., Quake, S. and Schere, A. (2003) 'Microfluidic integration on detector arrays for absorption and fluorescence micro-spectrometers', *Sensors and Actuators A: Physical*, Vol. 104, No. 1, pp.25–31.
- Aftab, D.T. and Hait, W.N. (1990) 'A semiautomated 96-well plate assay for protein Kinase C', *Analytical Biochemistry*, Vol. 187, No. 1, pp.84–88.
- Alberts, B.J.A., Lewis, J., Raff, M., Roberts, K. and Walter, P. (2002) *Molecular Biology of the Cell*, Garland Science.
- Antonov, V.F., Anosov, A.A., Norik, V.P. and Smirnova, E.Y. (2005) 'Soft perforation of planar bilayer lipid membranes of dipalmitoylphosphatidylcholine at the temperature of the phase transition from the liquid crystalline to the gel state', *Eur. Biophys. J.*, Vol. 34, No. 2, pp.155–162.

- Atanasov, V., Atanasova, P.P., Vockenroth, I.K., Knorr, N. and Koper, I. (2006) 'A molecular toolkit for highly insulating tethered bilayer lipid membranes on various substrates', *Bioconjugate Chemistry*, Vol. 17, No. 3, pp.631–637.
- Baaken, G., Ankri, N., Schuler, A-K., Rühle, J. and Behrends, J.C. (2011) 'Nanopore-based single-molecule mass spectrometry on a lipid membrane microarray', *ACS Nano.*, Vol. 5, No. 10, pp.8080–8088.
- Baldwin, R.L., Mirzabekov, T., Kagan, B.L. and Wisnieski, B.J. (1995) 'Conformation and ion channel activity of lymphotoxin at neutral and low pH', *J. Immunol.*, Vol. 154, No. 2, pp.790–798.
- Bechinger, B. (1997) 'Structure and functions of channel-forming peptides: magainins, cecropins, melittin and alamethicin', *Journal of Membrane Biology*, Vol. 156, No. 3, pp.197–211.
- Benachir, T. and Lafleur, M. (1995) 'Study of vesicle leakage induced by melittin', *Biochimica et Biophysica Acta (BBA) – Biomembranes*, Vol. 1235, No. 2, pp.452–460.
- Binks, B.P. and Rodrigues, J.A. (2005) 'Inversion of emulsions stabilized solely by ionizable nanoparticles', *Angewandte Chemie – International Edition*, Vol. 44, No. 3, pp.441–444.
- Buzea, C., Pacheco, I.I. and Robbie, K. (2007) 'Nanomaterials and nanoparticles: Sources and toxicity', *Biointerphases*, Vol. 2, No. 4, pp.MR17–MR71.
- Cedervall, T., Lynch, I., Lindman, S., Berggard, T., Thulin, E., Nilsson, H., Dawson, K.A. and Linse, S. (2007) 'Understanding the nanoparticle-protein corona using methods to quantify exchange rates and affinities of proteins for nanoparticles', *Proceedings of the National Academy of Sciences of the United States of America*, Vol. 104, No. 7, pp.2050–2055.
- Chatterjee, S. and Banerjee, D.K. (2002) 'Preparation, isolation, and characterization of liposomes containing natural and synthetic lipids', *Methods in Molecular Biology-Clifton then Totowa*, Vol. 199, pp.3–16.
- Chiou, C.T., Freed, V.H., Schmedding, D.W. and Kohnert, R.L. (1977) 'Partition-coefficient and bioaccumulation of selected organic chemicals', *Environmental Science & Technology*, Vol. 11, No. 5, pp.475–478.
- Chiou, C.T., Schmedding, D.W. and Manes, M. (1982) 'Partitioning of organic-compounds in octanol-water systems', *Environmental Science & Technology*, Vol. 16, No. 1, pp.4–10.
- Cooke, I.R., Kremer, K. and Deserno, M. (2005) 'Tunable generic model for fluid bilayer membranes', *Physical Review E*, Vol. 72, No. 1, p.011506.
- de Planque, M.R., Aghdaei, S., Roose, T. and Morgan, H. (2011) 'Electrophysiological characterization of membrane disruption by nanoparticles', *ACS Nano.*, Vol. 5, No. 5, pp.3599–3606.
- Deserno, M. (2009) 'Mesoscopic membrane physics: concepts, simulations, and selected applications', *Macromolecular Rapid Communications*, Vol. 30, Nos. 9–10, pp.752–771.
- Dulfer, W.J. and Govers, H.A.J. (1995) 'Membrane water partitioning of polychlorinated-biphenyls in small unilamellar vesicles of 4 saturated phosphatidylcholines', *Environmental Science & Technology*, Vol. 29, No. 10, pp.2548–2554.
- Dutt, M., Kuksenok, O., Nayhouse, M.J., Little, S.R. and Balazs, A.C. (2011) 'Modeling the self-assembly of lipids and nanotubes in solution: forming vesicles and bicelles with transmembrane nanotube channels', *ACS Nano.*, Vol. 5, No. 6, pp.4769–4782.
- Elimelech, M.J.X., Gregory, J. and Williams, R. (1998) *Particle Deposition & Aggregation: Measurement, Modelling and Simulation*, Butterworth-Heinemann.
- Escher, B.I. and Schwarzenbach, R.P. (1996) 'Partitioning of substituted phenols in liposome-water, biomembrane-water, and octanol-water systems', *Environmental Science & Technology*, Vol. 30, No. 1, pp.260–270.
- Eversmann, B., Jenkner, M., Hofmann, F., Paulus, C., Brederlow, R., Holzapfl, B., Fromherz, P., Merz, M., Brenner, M., Schreiter, M., Gabl, R., Plehnert, K., Steinhauser, M., Eckstein, G., Schmitt-Landsiedel, D. and Thewes, R. (2003) 'A 128 × 128 CMOS biosensor array for extracellular recording of neural activity', *IEEE Journal of Solid-State Circuits*, Vol. 38, No. 12, pp.2306–2317.

- Gao, H.J., Shi, W.D. and Freund, L.B. (2005) 'Mechanics of receptor-mediated endocytosis', *Proceedings of the National Academy of Sciences of the United States of America*, Vol. 102, No. 27, pp.9469–9474.
- García-Sáez, A.J. and Schwille, P. (2010) 'Surface analysis of membrane dynamics', *Biochimica et Biophysica Acta (BBA) – Biomembranes*, Vol. 1798, No. 4, pp.766–776.
- Genov, R., Stanacevic, M., Naware, M., Cauwenberghs, G. and Thakor, N. (2006) '16-channel integrated potentiostat for distributed neurochemical sensing', *IEEE Trans. Circuits Syst. I*, Vol. 53, No. 11, pp.2371–2376.
- Gervais, C., Dô, F., Cantin, A., Kukulj, G., White, P.W., Gauthier, A. and Vaillancourt, F.H. (2011) 'Development and validation of a high-throughput screening assay for the hepatitis C virus p7 viroporin', *Journal of Biomolecular Screening*, Vol. 16, No. 3, pp.363–369.
- Ginzburg, V.V. and Balijepalli, S. (2007) 'Modeling the thermodynamics of the interaction of nanoparticles with cell membranes', *Nano Letters*, Vol. 7, No. 12, pp.3716–3722.
- Giri, J., Diallo, M.S., Goddard, W.A., Dalleska, N.F., Fang, X.D. and Tang, Y.C. (2009) 'Partitioning of poly(amidoamine) dendrimers between n-octanol and water', *Environmental Science & Technology*, Vol. 43, No. 13, pp.5123–5129.
- Goodman, C.M., McCusker, C.D., Yilmaz, T. and Rotello, V.M. (2004) 'Toxicity of gold nanoparticles functionalized with cationic and anionic side chains', *Bioconjugate Chemistry*, Vol. 15, No. 4, pp.897–900.
- Gore, A., Chakrabarty, S., Pal, S. and Alocilja, E.C. (2006) 'A multichannel femtoampere-sensitivity potentiostat array for biosensing applications', *IEEE Trans. Circuits Syst. I*, Vol. 53, No. 11, pp.2357–2363.
- Hadjicharalambous, C., Sheynis, T., Jelinek, R., Shanahan, M.T., Ouellette, A.J. and Gizeli, E. (2008) 'Mechanisms of α -Defensin bactericidal action: comparative membrane disruption by cryptdin-4 and its disulfide-null analogue', *Biochemistry*, Vol. 47, No. 47, pp.12626–12634.
- Han, X.J., Studer, A., Sehr, H., Geissbuhler, I., di Berardino, M., Winkler, F.K. and Tiefenauer, L.X. (2007) 'Nanopore arrays for stable and functional free-standing lipid bilayers', *Advanced Materials*, Vol. 19, No. 24, pp.4466–4470.
- Helfrich, W. (1973) 'Elastic properties of lipid bilayers – theory and possible experiments', *Zeitschrift Fur Naturforschung C-a Journal of Biosciences*, Vol. C28, No. 11-1, pp.693–703.
- Herbig, M.E., Assi, F., Textor, M. and Merkle, H.P. (2006) 'The cell penetrating peptides pVEC and W2-pVEC induce transformation of gel phase domains in phospholipid bilayers without affecting their integrity', *Biochemistry*, Vol. 45, No. 11, pp.3598–3609.
- Hille, B. (1992) *Ionic Channels of Excitable Membranes*, Sinauer Associates Inc., Sunderland.
- Hirano, A., Uda, K., Maeda, Y., Akasaka, T. and Shiraki, K. (2010) 'One-dimensional protein-based nanoparticles induce lipid bilayer disruption: carbon nanotube conjugates and amyloid fibrils', *Langmuir*, Vol. 26, No. 22, pp.17256–17259.
- Hirano-Iwata, A., Aoto, K., Oshima, A., Taira, T., Yamaguchi, R.T., Kimura, Y. and Niwano, M. (2010a) 'Free-standing lipid bilayers in silicon chips-membrane stabilization based on microfabricated apertures with a nanometer-scale smoothness', *Langmuir*, Vol. 26, No. 3, pp.1949–1952.
- Hirano-Iwata, A., Oshima, A., Nasu, T., Taira, T., Kimura, Y. and Niwano, M. (2010b) 'Stable lipid bilayers based on micro- and nano-fabrication', *Supramolecular Chemistry*, Vol. 22, Nos.7–8, pp.406–412.
- Hirano-Iwata, A., Taira, T., Oshima, A., Kimura, Y. and Niwano, M. (2010c) 'Improved stability of free-standing lipid bilayers based on nanoporous alumina films', *Applied Physics Letters*, Vol. 96, No. 21, p.213706.
- Hirano-Iwata, A., Nasu, T., Oshima, A., Kimura, Y. and Niwano, M. (2012) 'Lipid bilayer array for simultaneous recording of ion channel activities', *Applied Physics Letters*, Vol. 101, No. 2, pp.023702–023703.

- Hladky, S.B. and Haydon, D.A. (1972) 'Ion transfer across lipid membranes in the presence of gramicidin A: I. Studies of the unit conductance channel', *Biochimica et Biophysica Acta (BBA) – Biomembranes*, Vol. 274, No. 2, pp.294–312.
- Hook, F., Stengel, G., Dahlin, A.B., Gunnarsson, A., Jonsson, M.P., Jonsson, P., Reimhult, E., Simonsson, L. and Svedhem, S. (2008) 'Supported lipid bilayers, tethered lipid vesicles, and vesicle fusion investigated using gravimetric, plasmonic, and microscopy techniques', *Biointerphases*, Vol. 3, No. 2, pp.FA108–FA116.
- Hope, M.J., Bally, M.B., Mayer, L.D., Janoff, A.S. and Cullis, P.R. (1986) 'Generation of multilamellar and unilamellar phospholipid vesicles', *Chemistry and Physics of Lipids*, Vol. 40, Nos.2–4, pp.89–107.
- Hou, W-C., Moghadam, B.Y., Corredor, C., Westerhoff, P. and Posner, J.D. (2012) 'Distribution of functionalized gold nanoparticles between water and lipid bilayers as model cell membranes', *Environmental Science & Technology*, Vol. 46, No. 3, pp.1869–1876.
- Hou, W-C., Moghadam, B.Y., Westerhoff, P. and Posner, J.D. (2011) 'Distribution of fullerene nanomaterials between water and model biological membranes', *Langmuir*, Vol. 27, No. 19, pp.11899–11905.
- Hristovski, K.D., Westerhoff, P.K. and Posner, J.D. (2011) 'Octanol-water distribution of engineered nanomaterials', *Journal of Environmental Science and Health Part A – Toxic/Hazardous Substances & Environmental Engineering*, Vol. 46, No. 6, pp.636–647.
- Hsiao, I.L. and Huang, Y.J. (2011) 'Titanium oxide shell coatings decrease the cytotoxicity of ZnO nanoparticles', *Chem. Res. Toxicol.*, Vol. 24, No. 3, pp.303–313.
- Im, H., Wittenberg, N.J., Lesuffleur, A., Lindquist, N.C. and Oh, S.H. (2010) 'Membrane protein biosensing with plasmonic nanopore arrays and pore-spanning lipid membranes', *Chemical Science*, Vol. 1, No. 6, pp.688–696.
- Jadhav, S.R. and Worden, R.M. (2008) 'Interaction of polyamidoamine (PAMAM) nanoparticles with the glassy carbon supported bilayer lipid membrane', *NSTI 2008*, 1–8 June 2008, NSTI, Boston, MA.
- Jadhav, S.R., Kota, S.R., Zheng, Y., Garavito, R.M. and Worden, R.M. (2012) 'Voltage dependent closure of PorB Class II porin from *Neisseria meningitidis* investigated using impedance spectroscopy in a tethered bilayer lipid membrane interface', *Journal of Colloid and Interface Science*, in press.
- Jadhav, S.R., Sui, D.X., Garavito, R.M. and Worden, R.M. (2008) 'Fabrication of highly insulating tethered bilayer lipid membrane using yeast cell membrane fractions for measuring ion channel activity', *J. Colloid Interface Sci.*, Vol. 322, No. 2, pp.465–472.
- Jafvert, C.T. and Kulkarni, P.P. (2008) 'Buckminsterfullerene's (C(60)) octanol-water partition coefficient (K(ow)) and aqueous solubility', *Environmental Science & Technology*, Vol. 42, No. 16, pp.5945–5950.
- Jafvert, C.T., Westall, J.C., Grieder, E. and Schwarzenbach, R.P. (1990) 'Distribution of hydrophobic ionogenic organic-compounds between octanol and water-organic-acids', *Environmental Science & Technology*, Vol. 24, No. 12, pp.1795–1803.
- Juska, A. (2008) 'Minimal models of multi-site ligand-binding kinetics', *Journal of Theoretical Biology*, Vol. 255, No. 4, pp.396–403.
- Jusufi, A., Devane, R.H., Shinoda, W. and Klein, M.L. (2011) 'Nanoscale carbon particles and the stability of lipid bilayers', *Soft Matter*, Vol. 7, No. 3, pp.1139–1146.
- Kelly, C.V., Leroueil, P.R., Orr, B.G., Holl, M.M.B. and Andricioaei, I. (2008) 'Poly(amidoamine) dendrimers on lipid bilayers II: effects of bilayer phase and dendrimer termination', *Journal of Physical Chemistry B*, Vol. 112, No. 31, pp.9346–9353.
- Kibrom, A., Roskamp, R.F., Jonas, U., Menges, B., Knoll, W., Paulsen, H. and Naumann, R.L.C. (2011) 'Hydrogel-supported protein-tethered bilayer lipid membranes: a new approach toward polymer-supported lipid membranes', *Soft Matter*, Vol. 7, No. 1, pp.237–246.

- Kichler, A., Mechtler, K., Behr, J-P. and Wagner, E. (1997) 'Influence of membrane-active peptides on lipospermine/DNA complex mediated gene transfer', *Bioconjugate Chemistry*, Vol. 8, No. 2, pp.213–221.
- Klaassen, C.D. (2007) *Casarett and Doull's Toxicology: The Basic Science of Poisons*, McGraw-Hill Professional.
- Klein, S.A., Wilk, S.J., Thornton, T.J. and Posner, J.D. (2008) 'Formation of nanopores in suspended lipid bilayers using quantum dots', *International Symposium on Advanced Nanodevices and Nanotechnology, Journal of Physics: Conference Series*, Institute of Physics Publishing, 012022.
- Kohli, N., Hassler, B.L., Parthasarathy, L., Richardson, R.J., Ofoli, R.Y., Worden, R.M. and Lee, I. (2006) 'Tethered lipid bilayers on electrolessly deposited gold for bioelectronic applications', *Biomacromolecules*, Vol. 7, No. 12, pp.3327–3335.
- Kresak, S., Hianik, T. and Naumann, R.L.C. (2009) 'Giga-seal solvent-free bilayer lipid membranes: from single nanopores to nanopore arrays', *Soft Matter*, Vol. 5, No. 20, pp.4021–4032.
- Krishna, G., Schulte, J., Cornell, B.A., Pace, R.J. and Osman, P.D. (2003) 'Tethered bilayer membranes containing ionic reservoirs: selectivity and conductance', *Langmuir*, Vol. 19, No. 6, pp.2294–2305.
- Kusonwiriawong, C., van de Wetering, P., Hubbell, J.A., Merkle, H.P. and Walter, E. (2003) 'Evaluation of pH-dependent membrane-disruptive properties of poly(acrylic acid) derived polymers', *European Journal of Pharmaceutics and Biopharmaceutics*, Vol. 56, No. 2, pp.237–246.
- Kwak, K.J., Valincius, G., Liao, W.C., Hu, X., Wen, X.J., Lee, A., Yu, B., Vanderah, D.J., Lu, W. and Lee, L.J. (2010) 'Formation and finite element analysis of tethered bilayer lipid structures', *Langmuir*, Vol. 26, No. 23, pp.18199–18208.
- Kwon, J.H., Liljestrand, H.M. and Katz, L.E. (2006) 'Partitioning of moderately hydrophobic endocrine disruptors between water and synthetic membrane vesicles', *Environmental Toxicology and Chemistry*, Vol. 25, No. 8, pp.1984–1992.
- Lee, H. and Larson, R.G. (2006) 'Molecular dynamics simulations of PAMAM dendrimer-induced pore formation in DPPC bilayers with a coarse-grained model', *Journal of Physical Chemistry B*, Vol. 110, No. 37, pp.18204–18211.
- Lee, H. and Larson, R.G. (2008) 'Coarse-grained molecular dynamics studies of the concentration and size dependence of fifth- and seventh-generation PAMAM dendrimers on pore formation in DMPC bilayer', *Journal of Physical Chemistry B*, Vol. 112, No. 26, pp.7778–7784.
- Lee, H. and Larson, R.G. (2009) 'Multiscale modeling of dendrimers and their interactions with bilayers and polyelectrolytes', *Molecules*, Vol. 14, No. 1, pp.423–438.
- Leroueil, P.R., Berry, S.A., Duthie, K., Han, G., Rotello, V.M., McNerny, D.Q., Baker, J.R., Orr, B.G. and Holl, M.M.B. (2008) 'Wide varieties of cationic nanoparticles induce defects in supported lipid bilayers', *Nano Letters*, Vol. 8, No. 2, pp.420–424.
- Leroueil, P.R., Hong, S.Y., Mecke, A., Baker, J.R., Orr, B.G. and Holl, M.M.B. (2007) 'Nanoparticle interaction with biological membranes: does nanotechnology present a janus face?', *Accounts of Chemical Research*, Vol. 40, No. 5, pp.335–342.
- Li, N., Harkema, J.R., Lewandowski, R.P., Wang, M., Bramble, L.A., Gookin, G.R., Ning, Z., Kleinman, M.T., Sioutas, C. and Nel, A.E. (2010) 'Ambient ultrafine particles provide a strong adjuvant effect in the secondary immune response: implication for traffic-related asthma flares', *Am. J. Physiol. Lung Cell Mol. Physiol.*, Vol. 299, No. 3, 18p.
- Lin, J.Q., Zhang, H.W., Chen, Z. and Zheng, Y.G. (2010) 'Penetration of lipid membranes by gold nanoparticles: insights into cellular uptake, cytotoxicity, and their relationship', *ACS Nano*, Vol. 4, No. 9, pp.5421–5429.

- Lundqvist, M., Stigler, J., Elia, G., Lynch, I., Cedervall, T. and Dawson, K.A. (2008) 'Nanoparticle size and surface properties determine the protein corona with possible implications for biological impacts', *Proceedings of the National Academy of Sciences of the United States of America*, Vol. 105, No. 58, pp.14265–14270.
- Lynch, I., Cedervall, T., Lundqvist, M., Cabaleiro-Lago, C., Linse, S. and Dawson, K.A. (2007) 'The nanoparticle – protein complex as a biological entity; a complex fluids and surface science challenge for the 21st century', *Advances in Colloid and Interface Science*, Vols. 134–135, pp.167–174.
- Lynch, I., Salvati, A. and Dawson, K.A. (2009) 'Protein-nanoparticle interactions what does the cell see?', *Nature Nanotechnology*, Vol. 4, No. 9, pp.546–547.
- MacDonald, R.C., MacDonald, R.I., Menco, B.P.M., Takeshita, K., Subbarao, N.K. and Hu, L-R. (1991) 'Small-volume extrusion apparatus for preparation of large, unilamellar vesicles', *Biochimica et Biophysica Acta (BBA) – Biomembranes*, Vol. 1061, No. 2, pp.297–303.
- Malmstadt, N., Nash, M.A., Purnell, R.F. and Schmidt, J.J. (2006) 'Automated formation of lipid-bilayer membranes in a microfluidic device', *Nano Letters*, Vol. 6, No. 9, pp.1961–1965.
- Manickam, A., Chevalier, A., McDermott, M., Ellington, A.D. and Hassibi, A. (2010) 'A CMOS electrochemical impedance spectroscopy (EIS) biosensor array', *IEEE Trans. Biomed. Circuits Syst.*, Vol. 4, No. 6, pp.379–390.
- Marrink, S.J., de Vries, A.H. and Mark, A.E. (2004) 'Coarse grained model for semiquantitative lipid simulations', *Journal of Physical Chemistry B*, Vol. 108, No. 2, pp.750–760.
- Marrink, S.J., Risselada, H.J., Yefimov, S., Tieleman, D.P. and de Vries, A.H. (2007) 'The MARTINI force field: coarse grained model for biomolecular simulations', *Journal of Physical Chemistry B*, Vol. 111, No. 27, pp.7812–7824.
- Matile, S., Berova, N. and Nakanishi, K. (1996) 'Exciton coupled circular dichroic studies of self-assembled brevetoxin-porphyrin conjugates in lipid bilayers and polar solvents', *Chem. Biol.*, Vol. 3, No. 5, pp.379–392.
- Matsuzaki, K., Yoneyama, S. and Miyajima, K. (1997) 'Pore formation and translocation of melittin', *Biophysical Journal*, Vol. 73, No. 2, pp.831–838.
- Mayer, L.D., Hope, M.J. and Cullis, P.R. (1986) 'Vesicles of variable sizes produced by a rapid extrusion procedure', *Biochimica et Biophysica Acta (BBA) – Biomembranes*, Vol. 858, No. 1, pp.161–168.
- Mecke, A., Majoros, I.J., Patri, A.K., Baker, J.R., Holl, M.M.B. and Orr, B.G. (2005) 'Lipid bilayer disruption by polycationic polymers: the roles of size and chemical functional group', *Langmuir*, Vol. 21, No. 33, pp.10348–10354.
- Mecke, A., Uppuluri, S., Sassanella, T.M., Lee, D.K., Ramamoorthy, A., Baker, J.R., Orr, B.G. and Holl, M.M.B. (2004) 'Direct observation of lipid bilayer disruption by poly(amidoamine) dendrimers', *Chemistry and Physics of Lipids*, Vol. 132, No. 1, pp.3–14.
- Min, M. and Parve, T. (2007) 'Improvement of lock-in bio-impedance analyzer for implantable medical devices', *IEEE Trans. Instrumentation and Measurement*, Vol. 56, No. 3, pp.968–974.
- Mironova, G.D., Skarga, Y.Y., Grigoriev, S.M., Negoda, A.E., Kolomytkin, O.V. and Marinov, B.S. (1999) 'Reconstitution of the mitochondrial ATP-dependent potassium channel into bilayer lipid membrane', *J. Bioenerg. Biomembr.*, Vol. 31, No. 2, pp.159–163.
- Moghadam, B.Y., Hou, W-C., Corredor, C., Westerhoff, P. and Posner, J.D. (2012) 'Role of nanoparticle surface functionality in the disruption of model cell membranes', *Langmuir*.
- Monticelli, L., Salonen, E., Ke, P.C. and Vattulainen, I. (2009) 'Effects of carbon nanoparticles on lipid membranes: a molecular simulation perspective', *Soft Matter*, Vol. 5, No. 22, pp.4433–4445.
- Mueller, P., Rudin, D.O., Tien, H.T. and Wescott, W.C. (1962) 'Reconstitution of cell membrane structure in vitro and its transformation into an excitable system', *Nature*, Vol. 194, pp.979–980.

- Muller, M., Katsov, K. and Schick, M. (2006) 'Biological and synthetic membranes: what can be learned from a coarse-grained description?', *Physics Reports-Review Section of Physics Letters*, Vol. 434, Nos. 5–6, pp.113–176.
- Muller, M.T., Zehnder, A.J.B. and Escher, B.I. (1999) 'Liposome-water and octanol-water partitioning of alcohol ethoxylates', *Environmental Toxicology and Chemistry*, Vol. 18, No. 10, pp.2191–2198.
- Neely, W.B., Branson, D.R. and Blau, G.E. (1974) 'Partition-coefficient to measure bioconcentration potential of organic chemicals in fish', *Environmental Science & Technology*, Vol. 8, No. 13, pp.1113–1115.
- Negoda, A., Xian, M. and Reusch, R.N. (2007) 'Insight into the selectivity and gating functions of *Streptomyces lividans* KcsA', *Proc. Natl. Acad. Sci., USA*, Vol. 104, pp.4342–4346.
- Nel, A., Xia, T., Madler, L. and Li, N. (2006) 'Toxic potential of materials at the nanolevel', *Science*, Vol. 311, No. 5761, pp.622–627.
- Nel, A.E., Madler, L., Velegol, D., Xia, T., Hoek, E.M.V., Somasundaran, P., Klaessig, F., Castranova, V. and Thompson, M. (2009) 'Understanding biophysicochemical interactions at the nano-bio interface', *Nature Materials*, Vol. 8, No. 7, pp.543–557.
- Nollert, P., Kiefer, H. and Jähnig, F. (1995) 'Lipid vesicle adsorption versus formation of planar bilayers on solid surfaces', *Biophysical Journal*, Vol. 69, No. 4, pp.1447–1455.
- Oberdorster, E., Zhu, S.Q., Blickey, T.M., McClellan-Green, P. and Haasch, M.L. (2006) 'Ecotoxicology of carbon-based engineered nanoparticles: effects of fullerene (C-60) on aquatic organisms', *Carbon*, Vol. 44, No. 6, pp.1112–1120.
- Oh, S.Y., Cornell, B., Smith, D., Higgins, G., Burrell, C.J. and Kok, T.W. (2008) 'Rapid detection of influenza A virus in clinical samples using an ion channel switch biosensor', *Biosensors and Bioelectronics*, Vol. 23, No. 3, pp.1161–1165.
- Oh-Hora, M. and Rao, A. (2008) 'Calcium signaling in lymphocytes', *Current Opinion in Immunology*, Vol. 20, No. 7, pp.250–258.
- Opperhuizen, A., Serne, P. and Vandersteen, J.M.D. (1988) 'Thermodynamics of fish water and octan-1-ol water partitioning of some chlorinated benzenes', *Environmental Science & Technology*, Vol. 22, No. 3, pp.286–292.
- Osaki, T., Suzuki, H., le Pioufle, B. and Takeuchi, S. (2009) 'Multichannel simultaneous measurements of single-molecule translocation in α -hemolysin nanopore array', *Analytical Chemistry*, Vol. 81, No. 24, pp.9866–9870.
- Osaki, T., Watanabe, Y., Kawano, R., Sasaki, H. and Takeuchi, S. (2011) 'Electrical access to lipid bilayer membrane microchambers transmembrane analysis', *Journal of Microelectromechanical Systems*, Vol. 20, No. 4, pp.797–799.
- Pavlov, E., Zakharian, E., Bladen, C., Diao, C.T., Grimbly, C., Reusch, R.N. and French, R.J. (2005) 'A large, voltage-dependent channel, isolated from mitochondria by water-free chloroform extraction', *Biophys. J.*, Vol. 88, No. 4, pp.2614–2625.
- Petersen, E.J., Huang, Q.G. and Weber, W.J. (2010) 'Relevance of octanol-water distribution measurements to the potential ecological uptake of multi-walled carbon nanotubes', *Environmental Toxicology and Chemistry*, Vol. 29, No. 5, pp.1106–1112.
- Prime, K.L. and Whitesides, G.M. (1991) 'Self-assembled organic monolayers: model systems for studying adsorption of proteins at surfaces', *Science*, Vol. 252, No. 1010, pp.1164–1167, New York, NY.
- Raguse, B., Braach-Maksvytis, V., Cornell, B.A., King, L.G., Osman, P.D.J., Pace, R.J. and Wiczorek, L. (1998) 'Tethered lipid bilayer membranes: formation and ionic reservoir characterization', *Langmuir*, Vol. 14, No. 3, pp.648–659.
- Ralston, E., Hjelmeland, L.M., Klausner, R.D., Weinstein, J.N. and Blumenthal, R. (1981) 'Carboxyfluorescein as a probe for liposome-cell interactions effect of impurities, and purification of the dye', *Biochimica et Biophysica Acta (BBA) – Biomembranes*, Vol. 649, No. 1, pp.133–137.

- Ramachandran, S., Merrill, N.E., Blick, R.H. and van der Weide, D.W. (2005) 'Colloidal quantum dots initiating current bursts in lipid bilayers', *Biosens Bioelectron*, Vol. 20, No. 10, pp.2173–2176.
- Rejman, J., Oberle, V., Zuhorn, I.S. and Hoekstra, D. (2004) 'Size-dependent internalization of particles via the pathways of clathrin-and caveolae-mediated endocytosis', *Biochemical Journal*, Vol. 377, pp.159–169.
- Rex, S. and Schwarz, G. (1998) 'Quantitative studies on the melittin-induced leakage mechanism of lipid vesicles', *Biochemistry*, Vol. 37, No. 8, pp.2336–2345.
- Robertson, J.W.F., Friedrich, M.G., Kibrom, A., Knoll, W., Naumann, R.L.C. and Walz, D. (2008) 'Modeling ion transport in tethered bilayer lipid membranes. 1. Passive ion permeation', *The Journal of Physical Chemistry B*, Vol. 112, No. 34, pp.10475–10482.
- Rossi, C. and Chopineau, J. (2007) 'Biomimetic tethered lipid membranes designed for membrane-protein interaction studies', *European Biophysics Journal*, Vol. 36, No. 8, pp.955–965.
- Ruta, V., Jiang, Y., Lee, A., Chen, J. and MacKinnon, R. (2003) 'Functional analysis of an archaeobacterial voltage-dependent K⁺ channel', *Nature*, Vol. 422, No. 6928, pp.180–185.
- Schienze, M., Paulus, C., Frey, A., Hofmann, F., Holzapfl, B., Schindler-Bauer, P. and Thewes, R. (2004) 'A fully electronic DNA sensor with 128 positions and in-pixel A/D conversion', *J. Solid-State Circuits*, Vol. 39, No. 12, pp.2438–2445.
- Schönherr, R., Hilger, M., Broer, S., Benz, R. and Braun, V. (1994) 'Interaction of serratia marcescens hemolysin (ShlA) with artificial and erythrocyte membranes. Demonstration of the formation of aqueous multistate channels', *Eur. J. Biochem.*, Vol. 223, No. 2, pp.655–663.
- Shelley, J.C., Shelley, M.Y., Reeder, R.C., Bandyopadhyay, S. and Klein, M.L. (2001) 'A coarse grain model for phospholipid simulations', *The Journal of Physical Chemistry B*, Vol. 105, No. 19, pp.4464–4470.
- Shinoda, W., Devane, R. and Klein, M.L. (2010) 'Zwitterionic lipid assemblies: molecular dynamics studies of monolayers, bilayers, and vesicles using a new coarse grain force field', *The Journal of Physical Chemistry B*, Vol. 114, No. 20, pp.6836–6849.
- Sila, M., Au, S. and Weiner, N. (1986) 'Effects of triton X-100 concentration and incubation temperature on carboxyfluorescein release from multilamellar liposomes', *Biochimica et Biophysica Acta (BBA) – Biomembranes*, Vol. 859, No. 2, pp.165–170.
- Studer, A., Han, X., Winkler, F.K. and Tiefenauer, L.X. (2009) 'Formation of individual protein channels in lipid bilayers suspended in nanopores', *Colloids Surf B Biointerfaces*, Vol. 73, No. 2, pp.325–331.
- Suzuki, H., Tabata, K.V., Noji, H. and Takeuchi, S. (2007) 'Electrophysiological recordings of single ion channels in planar lipid bilayers using a polymethyl methacrylate microfluidic chip', *Biosensors & Bioelectronics*, Vol. 22, No. 6, pp.1111–1115.
- Tao, X.J., Fortner, J.D., Zhang, B., He, Y.H., Chen, Y.S. and Hughes, J.B. (2009) 'Effects of aqueous stable fullerene nanocrystals (nC(60)) on *Daphnia magna*: evaluation of sub-lethal reproductive responses and accumulation', *Chemosphere*, Vol. 77, No. 11, pp.1482–1487.
- Teeguarden, J.G., Hinderliter, P.M., Orr, G., Thrall, B.D. and Pounds, J.G. (2007) 'Particokinetics in vitro: dosimetry considerations for in vitro nanoparticle toxicity assessments', *Toxicological Sciences*, Vol. 95, No. 2, pp.300–312.
- Terrettaz, S., Mayer, M. and Vogel, H. (2003) 'Highly electrically insulating tethered lipid bilayers for probing the function of ion channel proteins', *Langmuir*, Vol. 19, No. 14, pp.5567–5569.
- Tervonen, K., Waissi, G., Petersen, E.J., Akkanen, J. and Kukkonen, J.V.K. (2010) 'Analysis of fullerene-C(60) and kinetic measurements for its accumulation and depuration in *daphnia magna*', *Environmental Toxicology and Chemistry*, Vol. 29, No. 5, pp.1072–1078.
- Thei, F., Rossi, M., Bennati, M., Crescentini, M., Lodesani, F., Morgan, H. and Tartagni, M. (2010) 'Parallel recording of single ion channels: a heterogeneous system approach', *IEEE Transactions on Nanotechnology*, Vol. 9, No. 3, pp.295–302.

- Ti Tien, H. and Ottova-Leitmannova, A. (2000) *Membrane Biophysics as Viewed from Experimental Bilayer Lipid Membranes*, Elsevier Science, Amsterdam.
- Tiefenauer, L.X. and Studer, A. (2008) 'Nano for bio: nanopore arrays for stable and functional lipid bilayer membranes (mini review)', *Biointerphases*, Vol. 3, No. 2, pp.FA74–FA79.
- Titov, A.V., Kral, P. and Pearson, R. (2010) 'Sandwiched graphene-membrane superstructures', *ACS Nano.*, Vol. 4, No. 1, pp.229–234.
- Tosteson, M.T. and Tosteson, D.C. (1981) 'The sting. melittin forms channels in lipid bilayers', *Biophysical Journal*, Vol. 36, No. 1, pp.109–116.
- Tun, T.N. and Jenkins, A.T.A. (2010) 'An electrochemical impedance study of the effect of pathogenic bacterial toxins on tethered bilayer lipid membrane', *Electrochemistry Communications*, Vol. 12, No. 10, pp.1411–1415.
- van Lehn, R.C. and Alexander-Katz, A. (2011) 'Penetration of lipid bilayers by nanoparticles with environmentally-responsive surfaces: simulations and theory', *Soft Matter*, Vol. 7, No. 24, pp.11392–11404.
- Verma, A. and Stellacci, F. (2010) 'Effect of surface properties on nanoparticle-cell interactions', *Small*, Vol. 6, No. 1, pp.12–21.
- Wang, X., Xia, T.A., Ntim, S.A., Ji, Z.X., George, S., Meng, H.A., Zhang, H.Y., Castranova, V., Mitra, S. and Nel, A.E. (2010) 'Quantitative techniques for assessing and controlling the dispersion and biological effects of multiwalled carbon nanotubes in mammalian tissue culture cells', *ACS Nano.*, Vol. 4, No. 12, pp.7241–7252.
- White, R.J., Ervin, E.N., Yang, T., Chen, X., Daniel, S., Cremer, P.S. and White, H.S. (2007) 'Single ion-channel recordings using glass nanopore membranes', *J. Am. Chem. Soc.*, No. 129, pp.11766–11775.
- Wong-Ekkabut, J., Baoukina, S., Triampo, W., Tang, I.M., Tieleman, D.P. and Monticelli, L. (2008) 'Computer simulation study of fullerene translocation through lipid membranes', *Nature Nanotechnology*, Vol. 3, No. 6, pp.363–368.
- Yang, C. and Mason, A. (2009) 'Fully integrated 7-order frequency range quadrature sinusoid signal generator', *IEEE Trans. Instrumentation and Measurement*, Vol. 58, No. 10, pp.3481–3489.
- Yang, C., Huang, Y., Hassler, B.L., Worden, R.M. and Mason, A.J. (2009a) 'Amperometric electrochemical microsystem for a miniaturized protein biosensor array', *IEEE Trans. Biomedical Circ. Systems*, Vol. 3, No. 3, pp.160–168.
- Yang, C., Jadhav, S.R., Worden, M.R. and Mason, A.J. (2009b) 'Compact low power impedance-to-digital converter for sensor array microsystems', *IEEE J. Solid State Circuits*, Vol. 44, No. 10, pp.2844–2855.
- Yang, K. and Ma, Y.Q. (2010) 'Computer simulation of the translocation of nanoparticles with different shapes across a lipid bilayer', *Nature Nanotechnology*, Vol. 5, No. 8, pp.579–583.
- Yue, X., Drakakis, E.M., Lim, M., Radomska, A., Ye, H., Mantalaris, A., Panoskaltis, N. and Cass, A. (2008) 'A real-time multi-channel monitoring system for stem cell culture process', *IEEE Trans. Biomedical Circ. Systems*, Vol. 2, No. 2, pp.66–77.
- Yun, K.S., Kim, H.J., Joo, S., Kwak, J. and Yoon, E. (2000) 'Analysis of heavy metal ions using mercury microelectrodes and a solid-state reference electrode on a Si wafer', *Jpn. J. Appl. Phys. Part 1*, Vol. 39, pp.7159–7163.
- Zagnoni, M. (2012) 'Miniaturised technologies for the development of artificial lipid bilayer systems', *Lab on a Chip*, Vol. 12, No. 6, pp.1026–1039.
- Zagnoni, M., Sandison, M.E. and Morgan, H. (2009) 'Microfluidic array platform for simultaneous lipid bilayer membrane formation', *Biosensors & Bioelectronics*, Vol. 24, No. 5, pp.1235–1240.
- Zhu, X. and Ahn, C.H. (2006) 'On-chip electrochemical analysis system using nanoelectrodes and bioelectronic CMOS chip', *IEEE Sensors J.*, Vol. 6, No. 5, pp.1280–1286.